DEVELOPMENT OF CSMM-BASED SHELL ELEMENT FOR REINFORCED CONCRETE STRUCTURES

Presented

by

Y.L. Mo

February 8, 2017 at City University London, London, UK

Outline

1. Introduction
2. Formulation
3. Implementation
4. Validations
5. Nuclear Containment Vessels
6. Conclusions

1. Introduction

Offshore Platform

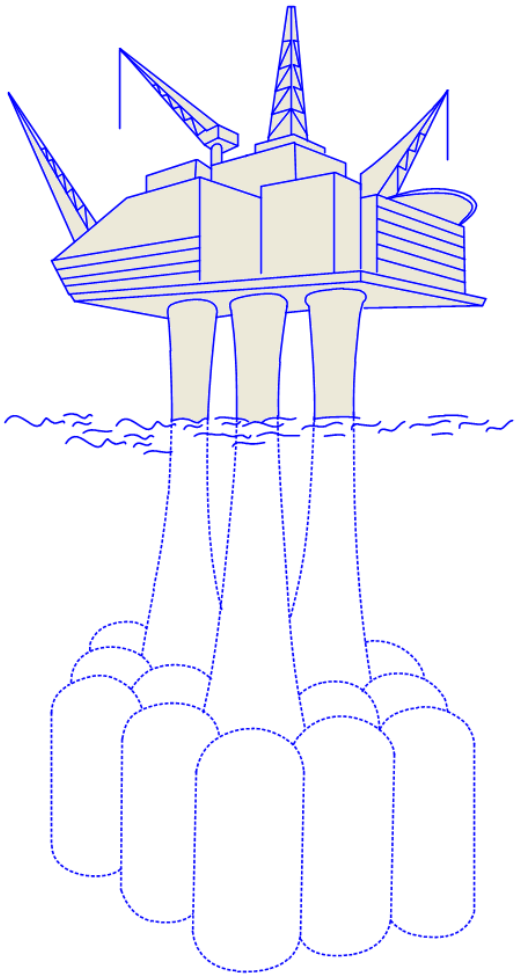

Dome Structure

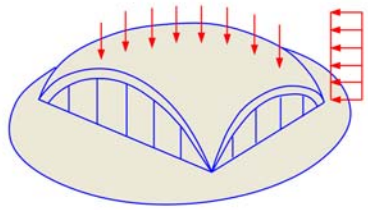

Nuclear Containment Vessel

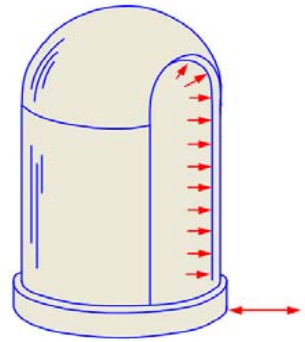

Cooling Tower

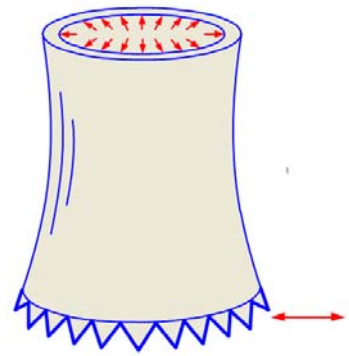

Coupling Shear Wall

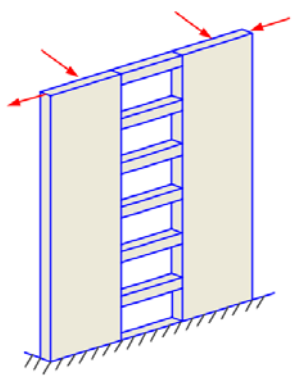

Box Bridge

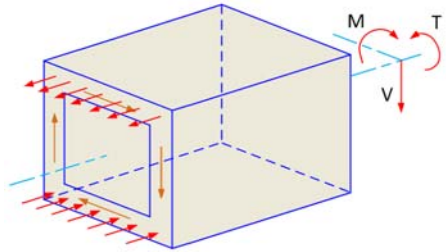

Core of High-Rise Building

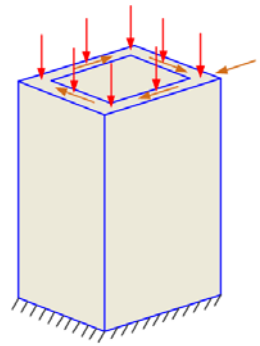

Reinforced Concrete Shell-Type Structures

1. Introduction

Opera House, Sydney, Australia (1973)
(www.wikipedia.org)

TWA Flight Center at JFK Airport, NYC (1962)
(www.wikipedia.org)

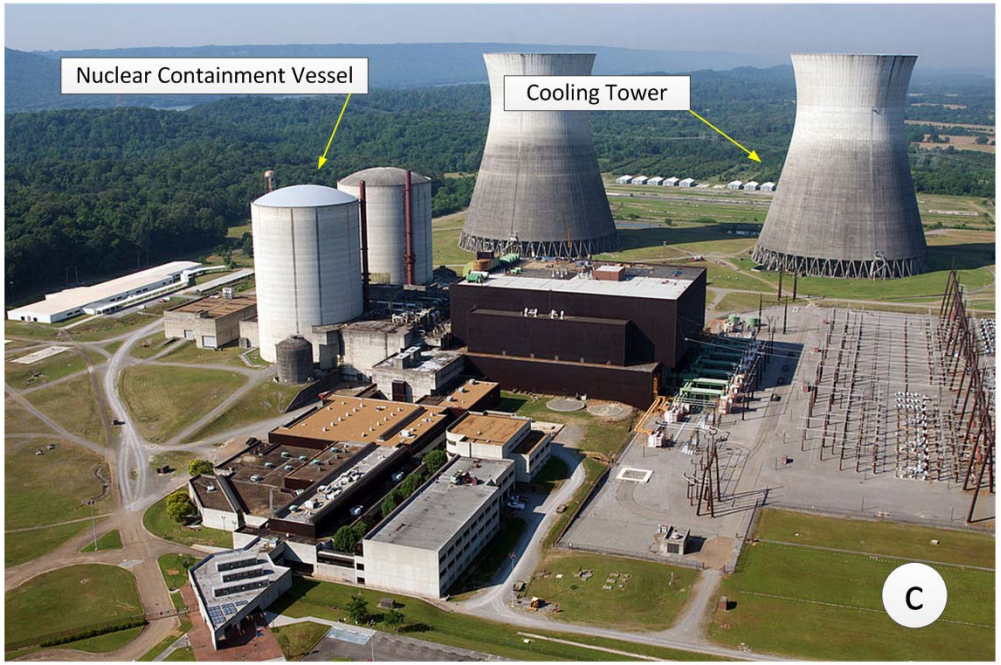

Modern RC shell structures in a nuclear power plant
(www.wikipedia.org)

1. Introduction

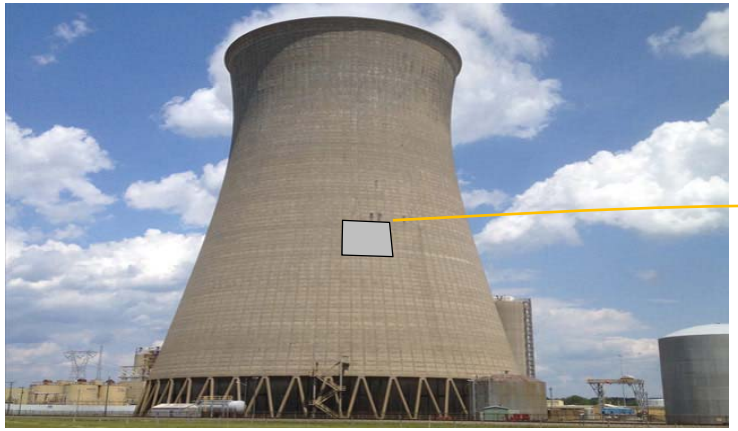

RC Shell Structures

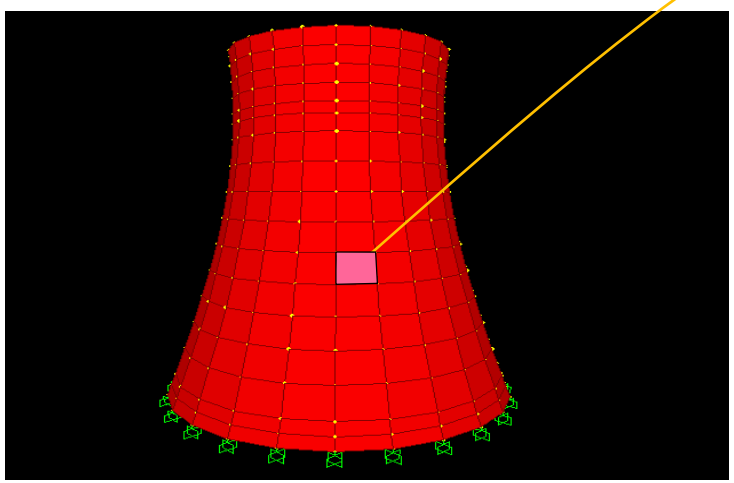

Modeling of RC Shell Structures

Finite element (FE) methods have been used successfully for the structural analysis of reinforced concrete shell structures over the decades.

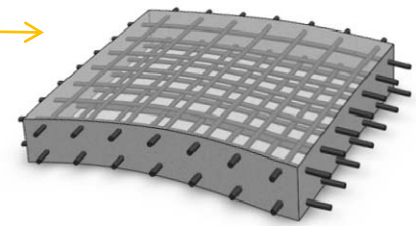

RC Shell Element

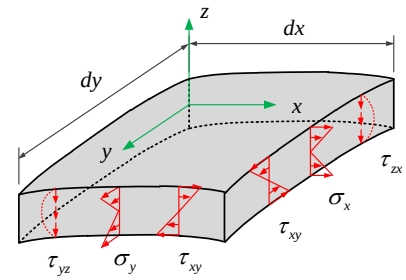

Stresses in Shell Element

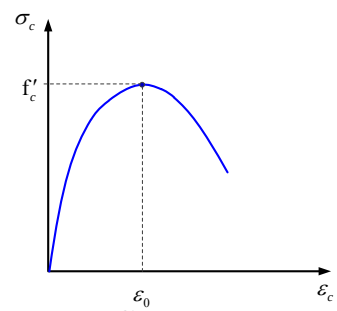

Concrete

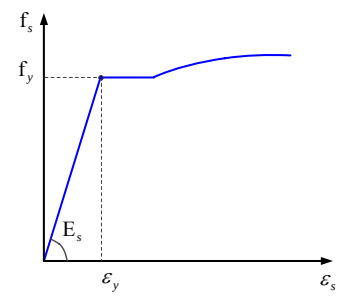

Steel Bar

Research Significantce

For an efficient FE analysis, it is necessary to have rational and effective numerical models for predicting accurately the structural behavior of large-scale RC shell structures.

1. Introduction

Research on RC Shell Structures using FEM

Year	Author	Organization
1972 1990	F.R. Hand, D.A. Pecknold, W.C. Schnobrich H.T. Hu & W.C. Schnobrich	University of Illinois, Urbana, USA
1984 1986	E. Hinton & D.R.J. Owen M. Cervera & E. Hinton	University College, Swansea, UK
1987	A.C. Scordelis & E.C. Chan	University of California, Berkeley, USA
1991 1993	Adebar & Collins M.A. Polak & F.J. Vecchio	University of Toronto, Canada
1997	P. Irawan & K. Maekawa	University of Tokyo, Japan
2002	T.H. Kim, K.M. Lee, H.M. Sin	Sungkyunkwan University, Korea
2006	Y.X. Zhang, M.A. Braford, R.I. Gilbert	University of New South Wales, Sydney, Australia
2012	H.J. Xiang, Y.L. Mo, T.T.C. Hsu	University of Houston, USA

1. Introduction

Select Element

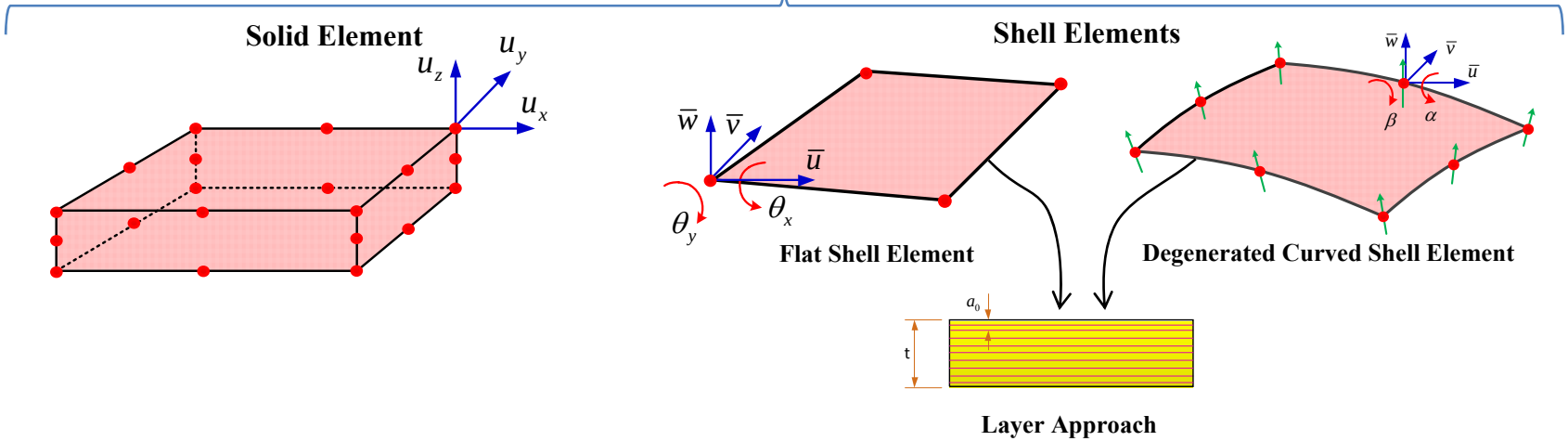

Develop Constitutive Models for RC

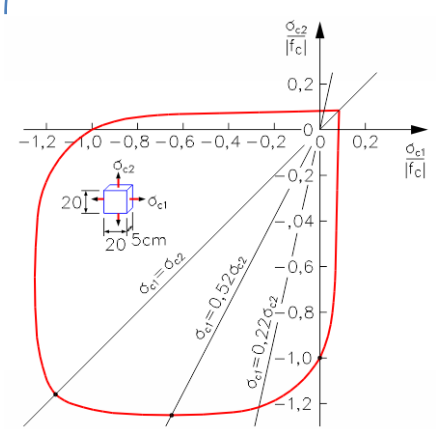

Biaxial Failure Curve (Kupfer, Hilsdorf, Rusch 1960)

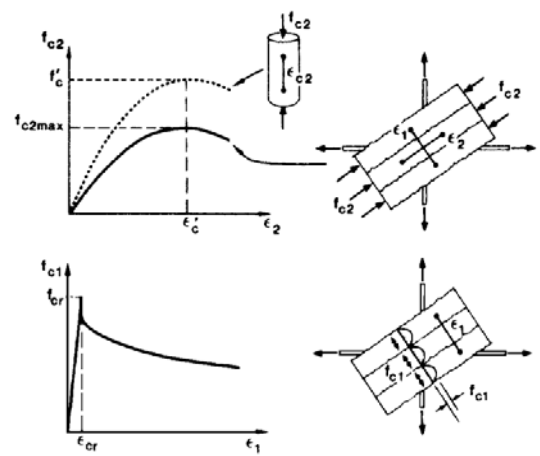

Compression Field Theory for Cracked Concrete (Vecchio & Collins, 1986)

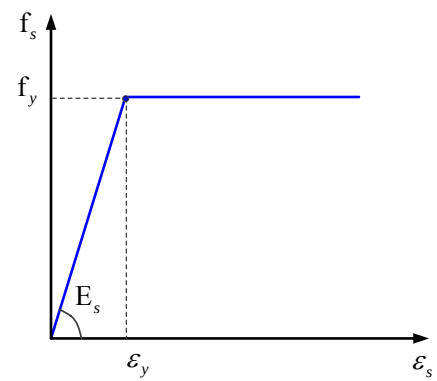

Constitutive Model for Mild Steel

1. Introduction

Universal Panel Tester (1988 - Now)

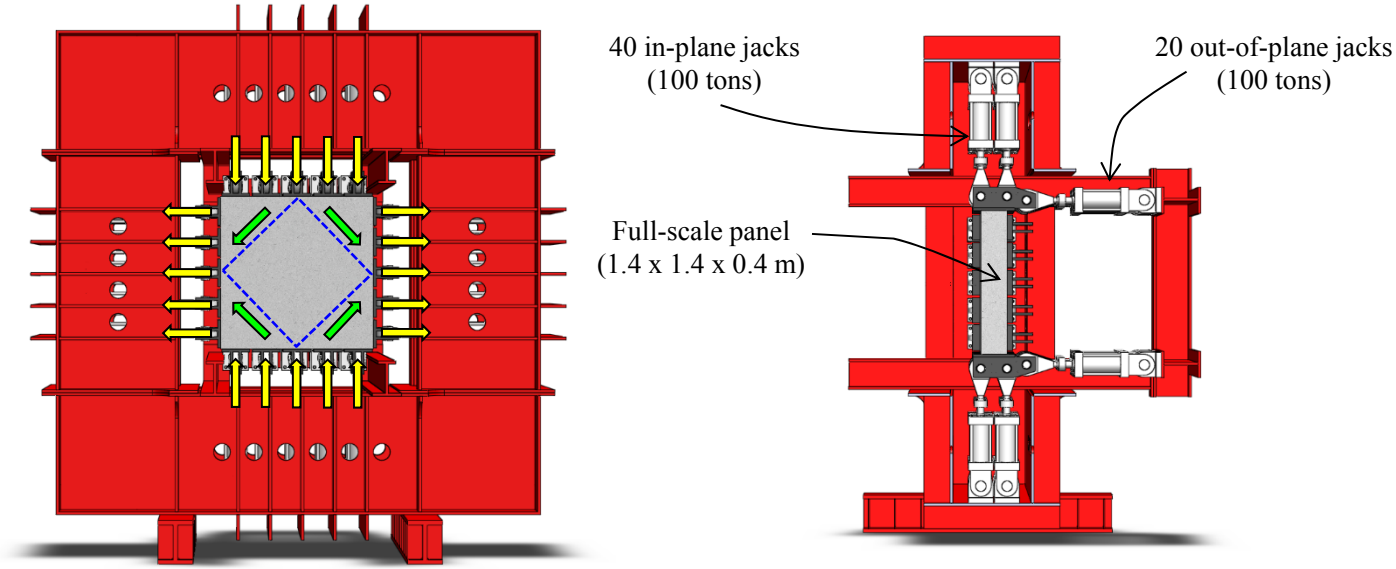

Front View **Cross Section**

Constitutive Models Developed at UH

(1) Rotating-Angle Softened Truss Model (RA-STM)

(2) Fixed-Angle Softened Truss Model (FA-STM)

(3) Softened Membrane Model (SMM)

(4) Cyclic Softened Membrane Model (CSMM)

(5) Cyclic Softened Membrane Model for Prestressed Concrete (CSMM-PC)

(6) Cyclic Softened Membrane Model for Prestressed Steel Fiber Concrete (CSMM-PSFC)

(7) Cyclic Softened Membrane Model for ECC (CSMM-ECC)

1. Introduction

Overview of Cyclic Softening Membrane Model (CSMM)

Cyclic Softening Membrane Model (CSMM)

- Uniaxial
  - Steel
  - Concrete
  - Softening Coefficient
- Biaxial
  - Hsu/Zhu Ratio
  - Shear

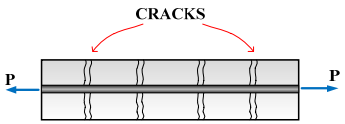

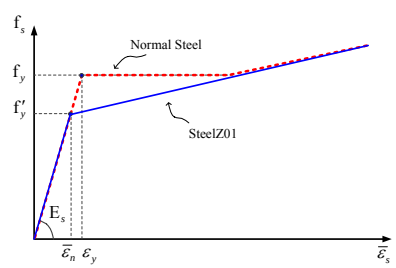

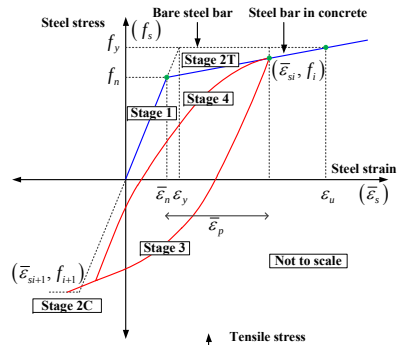

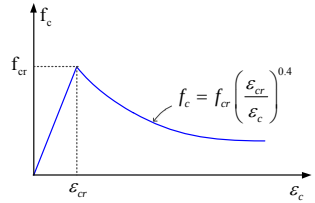

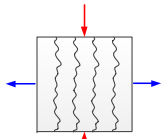

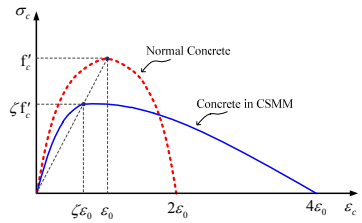

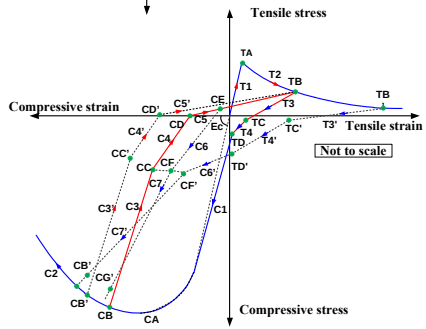

$$\zeta = \left(\frac{5.8}{\sqrt{f_c'(\text{MPa})}}\right)\left(\frac{1}{\sqrt{1+400\bar{\varepsilon}_T}}\right)\left(1-\frac{|\beta|}{24^o}\right) \le 0.9$$

Biaxial Strains ~ Uniaxial Strains $\varepsilon_1,\ \varepsilon_2,\ \varepsilon_{si}$ ⟹ $\bar{\varepsilon}_1,\ \bar{\varepsilon}_2,\ \bar{\varepsilon}_{si}$

$$[V] = \begin{bmatrix} \frac{1}{1-\nu_{12}\nu_{21}} & \frac{\nu_{12}}{1-\nu_{12}\nu_{21}} \\ \frac{\nu_{21}}{1-\nu_{12}\nu_{21}} & \frac{1}{1-\nu_{12}\nu_{21}} \end{bmatrix}$$

$$\nu_{12} = 0.2 + 850\varepsilon_{sf} \qquad \varepsilon_{sf} \le 0.002$$
$$\nu_{12} = 1.0 \qquad \varepsilon_{sf} > 0.002$$
$$\nu_{21} = 0.0$$

$$G_{12}^c = \frac{\left(\sigma_1^c - \sigma_2^c\right)}{2\left(\varepsilon_1 - \varepsilon_2\right)}$$

1. Introduction

Research on Finite Element Analysis (FE) at UH

Year	Authors	Developed Modules in OpenSees	Applications
2000	Jeng, Mo, and Hsu	Concrete J01 Steel J01	RC Beams, Columns
2005	Zhong, Mo, and Hsu	ConcreteZ01, ConcreteZ02 SteelZ01 FAFourSteelRCPlaneStress FAReinforceConcretePlaneStress	2-D RC Beams, Columns, Walls
2009	Laskar, Mo, and Hsu	ConcreteL01 TendonL01 FAPrestressConcretePlaneStress FAFourSteelPCPlaneStress	2-D PC Beams, Columns, Walls
2011	Rao, Mo, and Hsu	ConcreteR01	2-D PSFC Beams, Columns, Walls
2012	Xiang, Mo, and Hsu	FARCFiberShellX01	3D RC Walls
2013	Luu, Li, Mo, and Hsu	ConcreteECC01	2-D ECC Beams, Columns, Walls
2014	Tan, Mo, Hsu and Luu	ConcreteS01 Steel02 (Modified for Slipped Tendons)	PC Thin Slab Beams

OpenSees

An object-oriented software framework (C++) for simulation applications in earthquake engineering using finite element methods.

Key features of OpenSees include the interchangeability and the ability to integrate existing libraries and new components into the framework without changing the existing code.

OpenSees is open-source software. OpenSees is a research tool.

FE Program for Simulation of Concrete Structure (SCS)

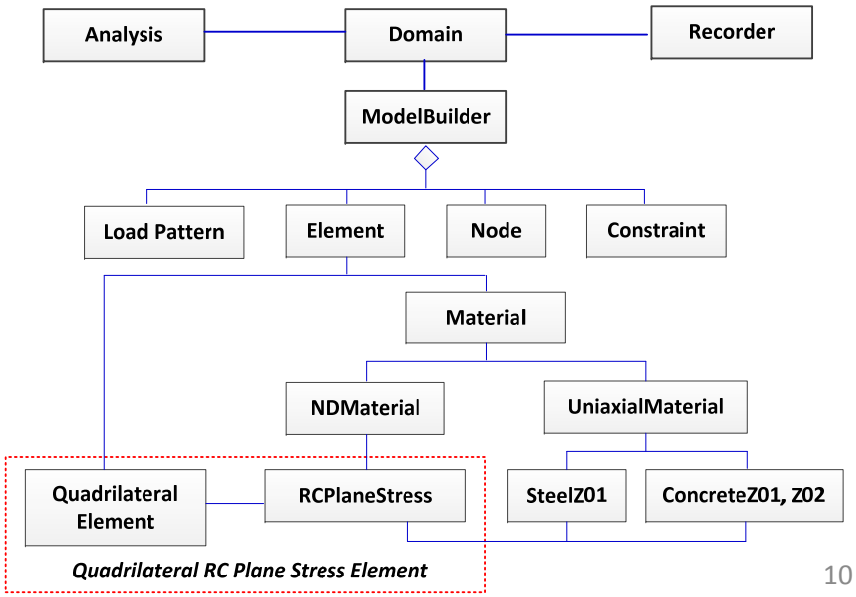

1. Introduction

Applications of SCS Program

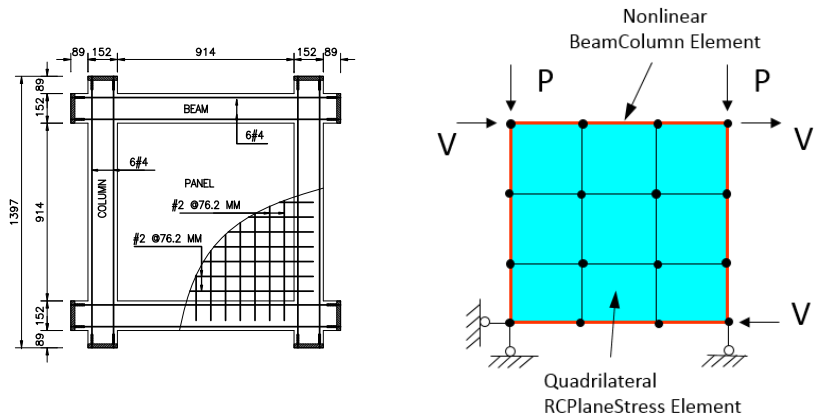

RC Frame and Shear Wall (Zhong, 2005)

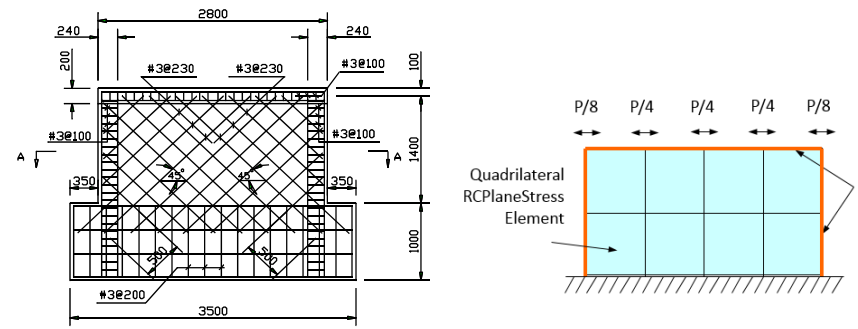

RC Shear Wall (Zhong, 2005)

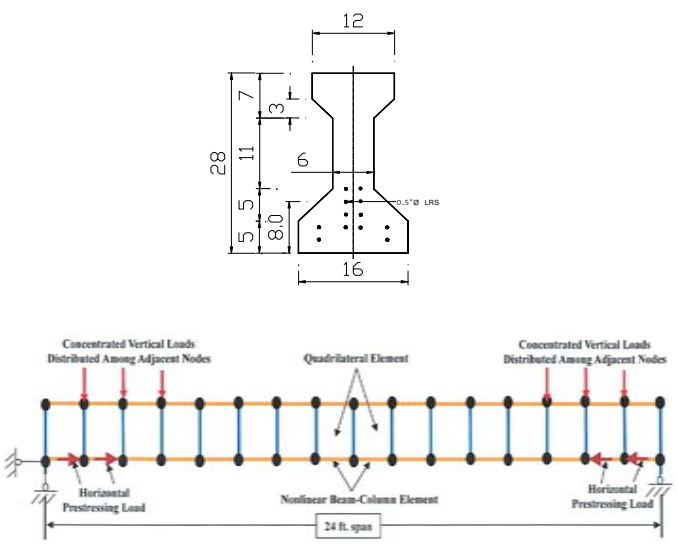

PC Girder (Laskar, 2009)

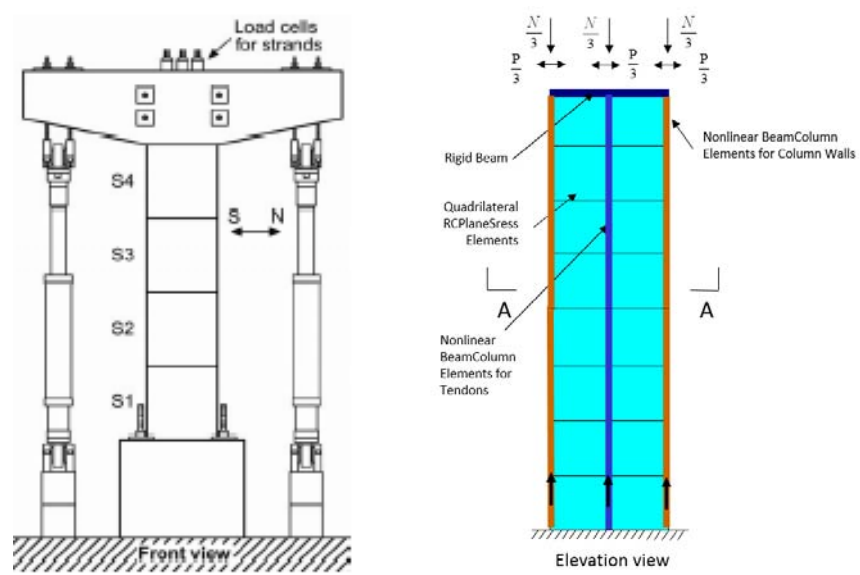

PC Bridge Column (Laskar, 2009)

1. Introduction

Research Objectives

- Develop a new shell element (named CSMMShellS8) based on the Cyclic Softened Membrane Model to formulate the degenerated shell theory with layered approach.

- Create a new finite element program (SCS-3D) with the developed shell element using OpenSees as a framework to predict the nonlinear behavior of RC structures.

- Validate the developed finite element program SCS-3D with several large-scale tests of RC shell structures subjected to reserved cyclic loadings.

- This research is undertaken as an international collaborative project between the National Center for Research on Earthquake Engineering (NCREE) and the University of Houston to investigate the inelastic behavior of RC nuclear containment vessels and two-story unsymmetrical RC building structures. The tests were performed at NCREE, and the design of the specimens and the study of the experimental results were performed at UH.

1. Introduction

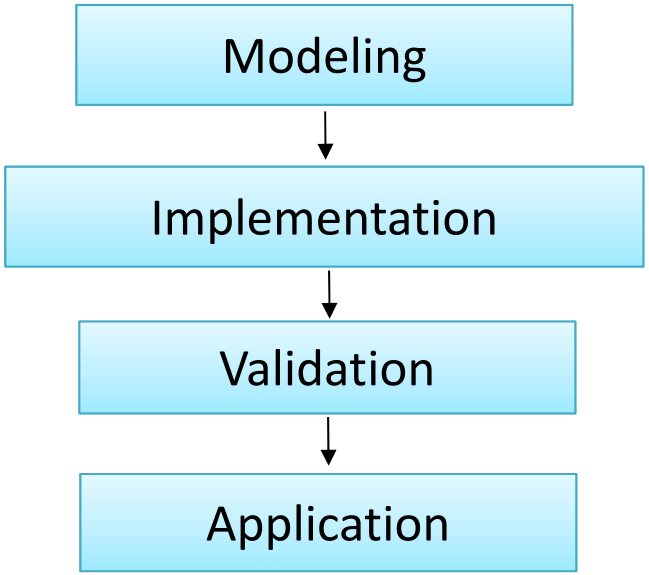

Model-Based Approach (MBS) is the basic methodology of this research.

2. Formulation

Element Selection

The **degenerated curved shell element** with layered approach has been recognized as the most promising element for analysis of RC curved shell structures since the 1970s. The element is derived from the equations of 3D continuum mechanics by reducing their dimensions in the thickness direction (Ahmad et al., 1970; Hughes, 1981; Hilton & Owen, 1984; Hu & Schnobrich, 1991; Cook, 2002)

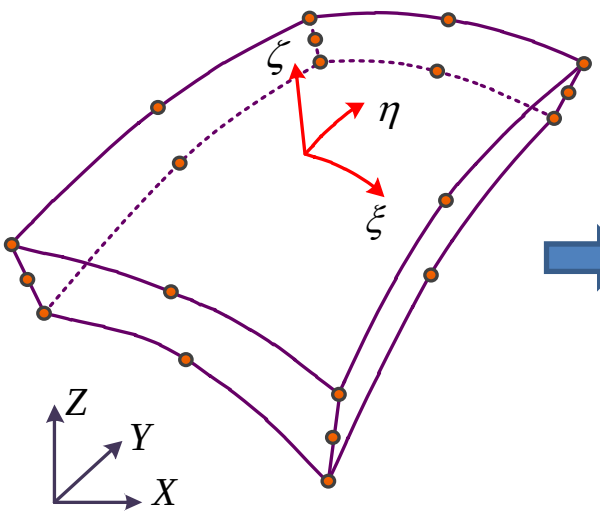

20-Node Solid Element

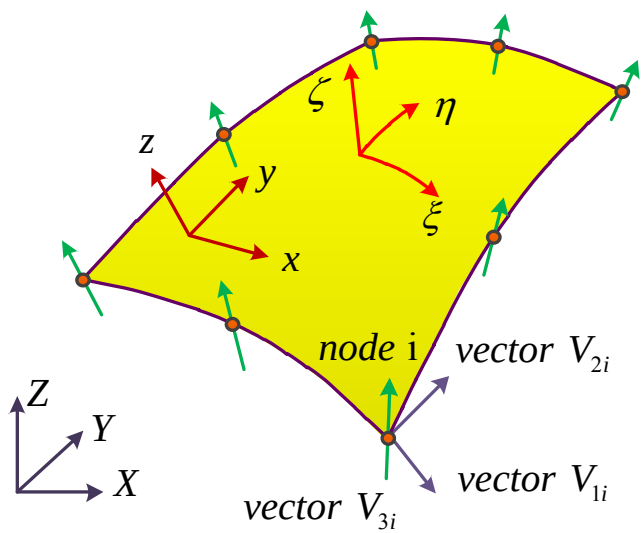

8-Node Degenerated Curved Shell Element

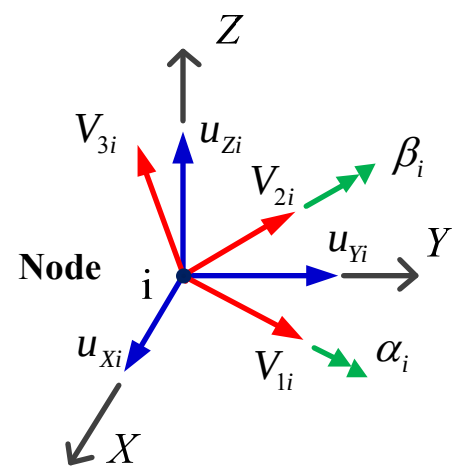

5 DOFs per node

X-Y-Z : Global coordinate system

ξ-η-ζ : Curvilinear coordinate system (xi, eta, zeta)

V_{1i}-V_{2i}-V_{3i} : Nodal coordinate system

x-y-z : Local coordinate system

2. Formulation

Fundamental Assumptions

1- A straight fiber that was perpendicular to the middle surface before deformation needs to remain straight but does not need to be perpendicular to the deformed middle surface (Mindlin theory)

$$\gamma_{xz} \neq 0 \qquad \gamma_{yz} \neq 0$$

2- Stresses normal to the mid-surface are negligible

$$\sigma_z = 0$$

3- Each shell layer remains in the plane stress state and the out-of-plane shear behavior are decoupled from the in-plane stresses and strains

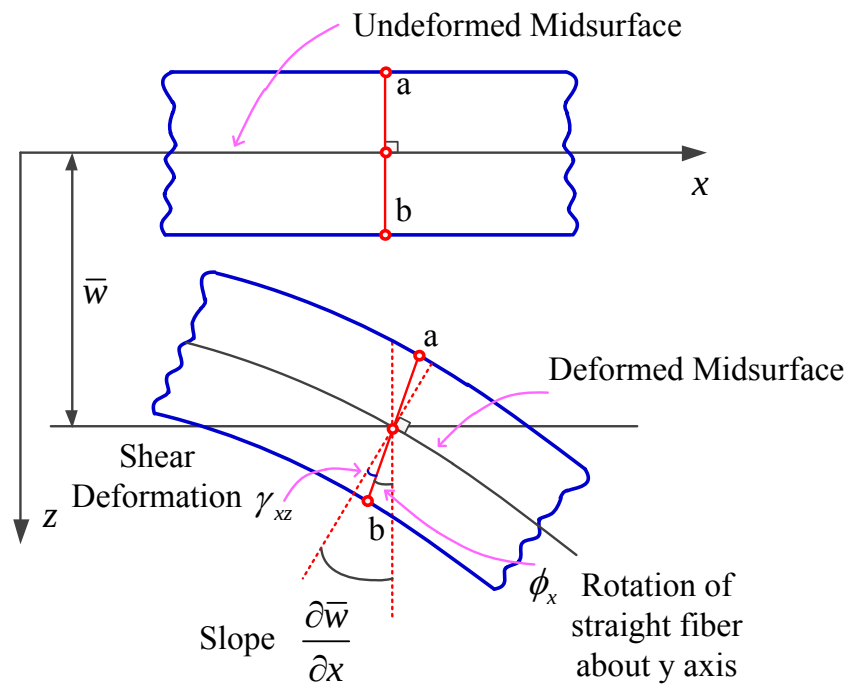

Element Stiffness Matrix

$$[k^e] = \int [B]^T [D][B] \; dV$$

[B]: matrix representing the shape functions

➡ ***Element Formulation***

[D]: constitutive material matrix

➡ ***Constitutive Material Formulation***
(CSMM)

2. Formulation

Element Geometry

$$\begin{Bmatrix} X \\ Y \\ Z \end{Bmatrix} = \sum N_i(\xi,\eta)\begin{Bmatrix} X_i \\ Y_i \\ Z_i \end{Bmatrix} + \sum N_i(\xi,\eta)\zeta\frac{t_i}{2}\begin{Bmatrix} l_{3i} \\ m_{3i} \\ n_{3i} \end{Bmatrix} \qquad \text{(Eq. 3.3)}$$

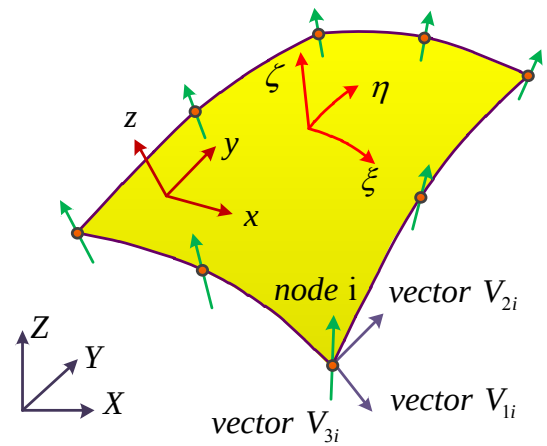

The Displacement Field

$$\begin{Bmatrix} u_X \\ u_Y \\ u_Z \end{Bmatrix} = \sum_{i=1}^{n\ node} N_i(\xi,\eta)\left[\begin{Bmatrix} u_{Xi} \\ u_{Yi} \\ u_{Zi} \end{Bmatrix} + \frac{1}{2}\zeta t_i\left[-\frac{V_{2i}}{|V_{2i}|},\frac{V_{1i}}{|V_{1i}|}\right]\begin{Bmatrix} \alpha_i \\ \beta_i \end{Bmatrix}\right] \Longleftrightarrow \underset{3x1}{\left\{u|_{\xi,\eta,\zeta}\right\}} = \underset{3x40}{\left[N(\xi,\eta,\zeta)\right]}\underset{40x1}{\left\{U^e\right\}} \qquad \text{(Eq. 3.5)}$$

$$\Longrightarrow \underset{9x1}{\left\{\partial u|_{\xi,\eta,\zeta}\right\}} = \underset{9x40}{\left[\partial N(\xi,\eta,\zeta)\right]}\underset{40x1}{\left\{U^e\right\}} \qquad \text{(Eq. 3.11)}$$

$$\underset{9x1}{\left\{\partial u|_{X,Y,Z}\right\}} = \underset{9x9}{\left[J_0\right]^{-1}}\underset{9x1}{\left\{\partial u|_{\xi,\eta,\zeta}\right\}} = \underset{9x9}{\left[J_0\right]^{-1}}\underset{9x40}{\left[\partial N(\xi,\eta,\zeta)\right]}\underset{40x1}{\left\{U^e\right\}} \qquad \text{(Eq. 3.9)} \Longrightarrow$$

To calculate strains

$\left\{U^e\right\}$ is the displacement vector of the shell element $\left\{U^e\right\} = \left\{u_{X1}, u_{Y1}, u_{Z1}, \alpha_1, \beta_1, \ldots, u_{Xn}, u_{Yn}, u_{Zn}, \alpha_n, \beta_n\right\}^T$

$N_i(\xi,\eta)$ is 2D shape function at node i $\quad \left[J_0\right]^{-1}$ is Jacobian matrix (Eq. 3.23)

2. Formulation

The Strain-Displacement Relationship

$$\varepsilon_X = \frac{\partial u_X}{\partial X}; \quad \varepsilon_Y = \frac{\partial u_Y}{\partial Y}; \quad \varepsilon_Z = \frac{\partial u_Z}{\partial Z}; \quad \gamma_{XZ} = \frac{\partial u_X}{\partial Z} + \frac{\partial u_Z}{\partial X}; \quad \gamma_{YZ} = \frac{\partial u_Y}{\partial Z} + \frac{\partial u_Z}{\partial Y}; \quad \gamma_{XY} = \frac{\partial u_X}{\partial Y} + \frac{\partial u_Y}{\partial X};$$

$$\Leftrightarrow \quad \underset{6\text{x}1}{\left\{\varepsilon\,|_{X,Y,Z}\right\}} = \underset{6\text{x}9}{[\mathrm{H}]}\underset{9\text{x}1}{\left\{\partial u\,|_{X,Y,Z}\right\}} \quad \text{(Eq. 3.7)}$$

Combining Eqs (3.7 & 3.9) gives $\underset{6\text{x}1}{\{\varepsilon\}} = \left(\underset{6\text{x}9}{[\mathrm{H}]}\underset{9\text{x}9}{[\mathrm{J}_0]^{-1}}\underset{9\text{x}40}{\left[\partial N(\xi,\eta,\zeta)\right]}\right)\underset{40\text{x}1}{\{U^e\}} = \underset{6\text{x}40}{[B]}\underset{40\text{x}1}{\{U^e\}}$ (Eq. 3.12)

$\underset{6\text{x}40}{[B]} = \underset{6\text{x}9}{[\mathrm{H}]}\underset{9\text{x}9}{[\mathrm{J}_0]^{-1}}\underset{9\text{x}40}{\left[\partial N(\xi,\eta,\zeta)\right]}$ is strain-displacement relation matrix

Element Stiffness Matrix & Element Internal Force Vector

$$\underset{40\times40}{[\mathrm{k}^e]} = \int \underset{40\times6}{[\mathrm{B}]^T}\underset{6\times6}{[\mathrm{D}\,|_{X,Y,Z}]}\underset{6\times40}{[\mathrm{B}]}\,\mathrm{d}V \quad \& \quad \underset{40\times1}{[\mathrm{f}^e]} = \int \underset{40\times6}{[\mathrm{B}]^T}\underset{6\times1}{\left\{\sigma\,|_{X,Y,Z}\right\}}\,\mathrm{d}V$$

$\mathrm{d}V = dx\,dy\,dz = \det[\mathrm{J}]\,\mathrm{d}\xi\,\mathrm{d}\eta\,\mathrm{d}\zeta$ is the element volume

$[\mathrm{D}\,|_{X,Y,Z}]$ is the global constitutive material matrix

2. Formulation

Constitutive Material Model

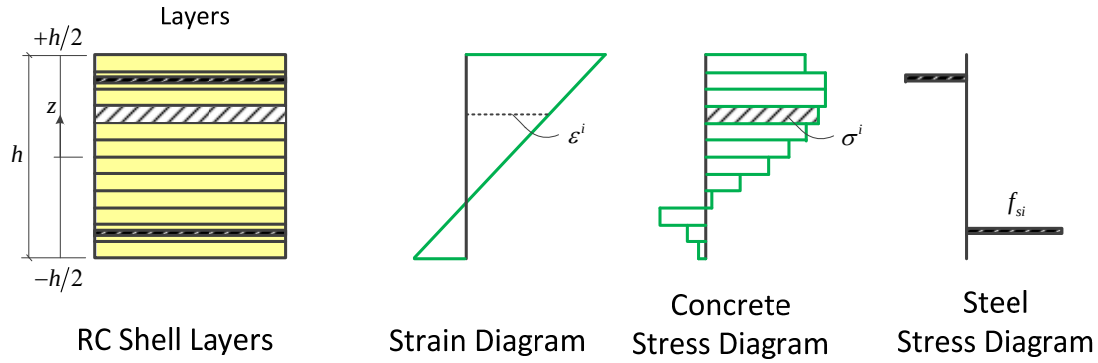

In the global coordinate: $\{\sigma|_{X,Y,Z}\} = [\mathrm{D}|_{X,Y,Z}]\{\varepsilon|_{X,Y,Z}\}$

In the local coordinate: $\{\sigma|_{x,y,z}\} = [\mathrm{D}|_{x,y,z}]\{\varepsilon|_{x,y,z}\}$

$$\begin{Bmatrix} \sigma_x \\ \sigma_y \\ \tau_{xy} \\ \sigma_z \\ \tau_{xz} \\ \tau_{yz} \end{Bmatrix} = \begin{bmatrix} & & & 0 & 0 & 0 \\ & D_{in} & & 0 & 0 & 0 \\ & & & 0 & 0 & 0 \\ 0 & 0 & 0 & 0 & 0 & 0 \\ 0 & 0 & 0 & 0 & & \\ 0 & 0 & 0 & 0 & D_{out} & \end{bmatrix} \begin{Bmatrix} \varepsilon_x \\ \varepsilon_y \\ \gamma_{xy} \\ \varepsilon_z \\ \gamma_{xz} \\ \gamma_{yz} \end{Bmatrix}$$

$$[\mathrm{D}|_{X,Y,Z}] = [T_\varepsilon]^T [\mathrm{D}|_{x,y,z}][T_\varepsilon]$$

$$[T_\varepsilon] = \begin{bmatrix} l_1^2 & m_1^2 & n_1^2 & l_1 m_1 & m_1 n_1 & n_1 l_1 \\ l_2^2 & m_2^2 & n_2^2 & l_2 m_2 & m_2 n_2 & n_2 l_2 \\ l_3^2 & m_3^2 & n_3^2 & l_3 m_3 & m_3 n_3 & n_3 l_3 \\ 2l_1 l_2 & 2m_1 m_2 & 2n_1 n_2 & l_1 m_2 + l_2 m_1 & m_1 n_2 + m_2 n_1 & n_1 l_2 + n_2 l_1 \\ 2l_2 l_3 & 2m_2 m_3 & 2n_2 n_3 & l_2 m_3 + l_3 m_2 & m_2 n_3 + m_3 n_2 & n_2 l_3 + n_3 l_2 \\ 2l_3 l_1 & 2m_3 m_1 & 2n_3 n_1 & l_3 m_1 + l_1 m_3 & m_3 n_1 + m_1 n_3 & n_1 l_2 + n_1 l_3 \end{bmatrix}$$

	X	Y	Z
x	l_1	m_1	n_1
y	l_2	m_2	n_2
z	l_3	m_3	n_3

Implementation of CSMM

In-plane:

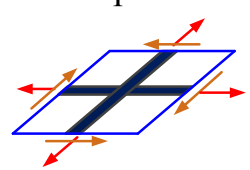

$$\begin{Bmatrix} \sigma_x \\ \sigma_y \\ \tau_{xy} \end{Bmatrix} = \begin{bmatrix} & & \\ & D_{in} & \\ & & \end{bmatrix} \begin{Bmatrix} \varepsilon_x \\ \varepsilon_y \\ \gamma_{xy} \end{Bmatrix}$$

Out-of-plane:

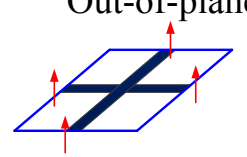

$$\begin{Bmatrix} \tau_{xz} \\ \tau_{yz} \end{Bmatrix} = \begin{bmatrix} D_{out} \end{bmatrix} \begin{Bmatrix} \gamma_{xz} \\ \gamma_{yz} \end{Bmatrix}$$

2. Formulation

Formulation of CSMM for Shell Element

Coordinate Systems for CSMM

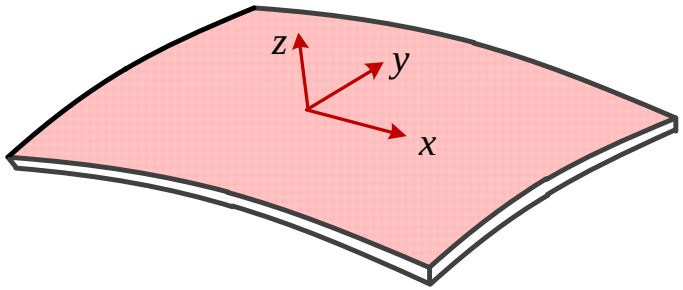

Concrete Layer

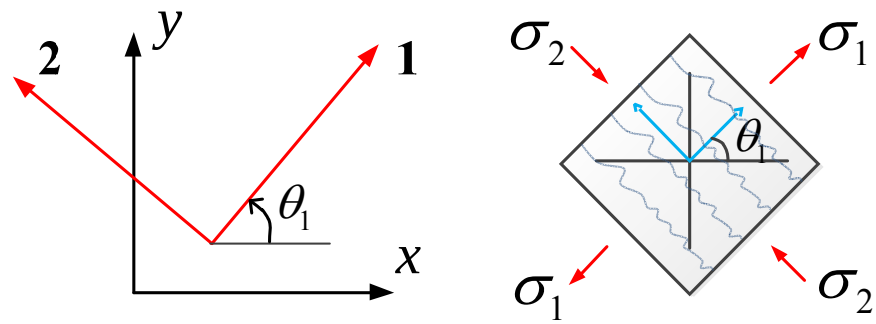

1-2: Orientation of Principal Stress

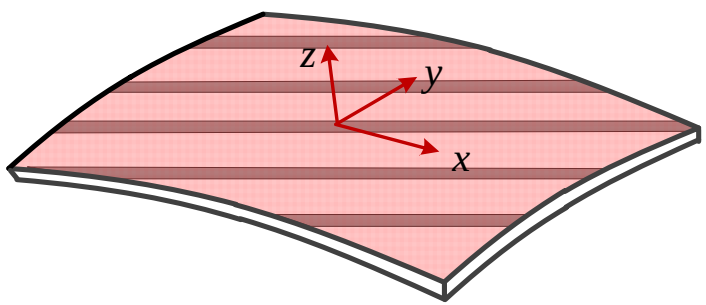

Steel Layer

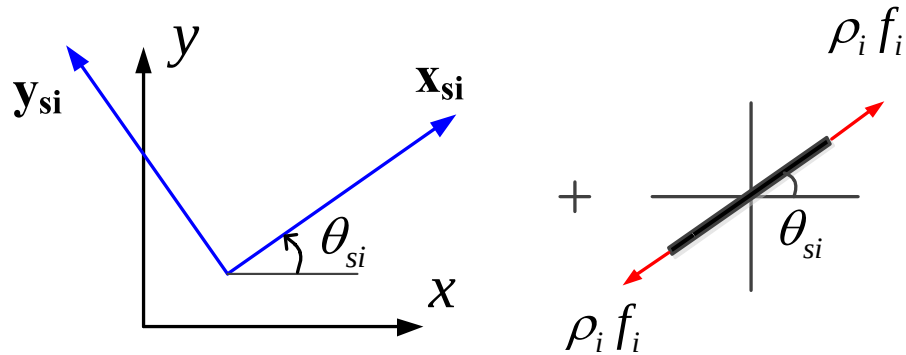

x_{si}-y_{si}: Orientation of Steel Bar

2. Formulation

Formulation of CSMM for Shell Element (Cont.)

Compatibility Equations

$$\begin{Bmatrix}\varepsilon_1\\ \varepsilon_2\\ \gamma_{12}\end{Bmatrix}=\left[\mathrm{T}_\varepsilon(\theta_1)\right]\begin{Bmatrix}\varepsilon_x\\ \varepsilon_y\\ \gamma_{xy}\end{Bmatrix}$$

Concrete Layer

$$\begin{Bmatrix}\varepsilon_{si}\\ \varepsilon_{si'}\\ 0\end{Bmatrix}=\left[\mathrm{T}_\varepsilon(\theta_{si}-\theta_1)\right]\begin{Bmatrix}\varepsilon_1\\ \varepsilon_2\\ \gamma_{12}\end{Bmatrix}$$

Steel Layer

Biaxial Strains ~ Uniaxial Strains

$$\varepsilon_1,\ \varepsilon_2,\ \varepsilon_{si} \Rightarrow \bar{\varepsilon}_1,\ \bar{\varepsilon}_2,\ \bar{\varepsilon}_{si}$$

Constitutive Laws of Uniaxial Materials

$$\bar{\varepsilon}_1,\ \bar{\varepsilon}_2,\ \gamma_{12} \Rightarrow \sigma_1^c,\ \bar{E}_1^c,\ \sigma_1^c,\ \bar{E}_1^c,\ G_{12}^c,\ \tau_{12}^c$$

$$\bar{\varepsilon}_{si} \Rightarrow f_{si},\ \bar{E}_{si}$$

Equilibrium Equations

$$\begin{Bmatrix}\sigma_x\\ \sigma_y\\ \tau_{xy}\end{Bmatrix}=\left[\mathrm{T}_\varepsilon(\theta_1)\right]^{-T}\begin{Bmatrix}\sigma_1^c\\ \sigma_2^c\\ \tau_{12}^c\end{Bmatrix}$$

Concrete Layer

$$\begin{Bmatrix}\sigma_x\\ \sigma_y\\ \tau_{xy}\end{Bmatrix}=\sum\left[\mathrm{T}_\varepsilon(\theta_{si})\right]^{-T}\begin{Bmatrix}f_{si}\\ 0\\ 0\end{Bmatrix}$$

Steel Layer

$$\left[\overline{D_{in}}\right]$$

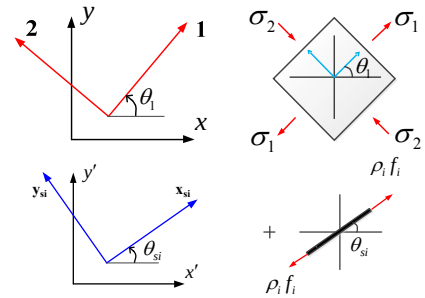

$$\left[\mathrm{T}_\varepsilon(\alpha)\right]=\begin{bmatrix}c^2 & s^2 & sc\\ s^2 & c^2 & -sc\\ -2sc & 2sc & c^2-s^2\end{bmatrix}$$

$$c=\cos(\alpha) \qquad s=\sin(\alpha)$$

$$[V]=\begin{bmatrix}\dfrac{1}{1-\nu_{12}\nu_{21}} & \dfrac{\nu_{12}}{1-\nu_{12}\nu_{21}}\\ \dfrac{\nu_{21}}{1-\nu_{12}\nu_{21}} & \dfrac{1}{1-\nu_{12}\nu_{21}}\end{bmatrix}$$

$$\nu_{12}=0.2+850\varepsilon_{sf} \qquad \varepsilon_{sf}\le 0.002$$

$$\nu_{12}=1.0 \qquad \varepsilon_{sf}>0.002$$

$$\nu_{21}=0.0$$

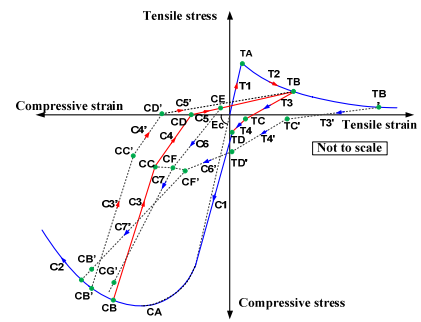

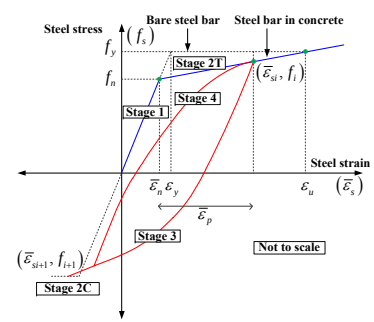

(Mansour and Hsu, 2005)

(Mo, Zhong, and Hsu 2008)

2. Formulation

Formulation of CSMM for Shell Element (Cont.)

In-plane:

Concrete Layer

$$\left[\overline{D_{in}}\right]=\begin{bmatrix} \bar{E}_1^c & \dfrac{\partial\sigma_1^c}{\partial\bar{\varepsilon}_2} & 0 \\ \dfrac{\partial\sigma_1^c}{\partial\bar{\varepsilon}_2} & \bar{E}_2^c & 0 \\ 0 & 0 & G_{12}^c \end{bmatrix}$$

$\bar{E}_1^c$; $\bar{E}_2^c$ are the uniaxial tangent moduli of concrete in the principal stress directions.

$\dfrac{\partial\sigma_1^c}{\partial\bar{\varepsilon}_2}$; $\dfrac{\partial\sigma_1^c}{\partial\bar{\varepsilon}_2}$ can be obtained by the uniaxial constitutive relationships and taking into account the stress/strain state of concrete.

G_{12}^c shear modulus of concrete, taken as $\left(\sigma_1^c-\sigma_2^c\right)/2\left(\varepsilon_1-\varepsilon_2\right)$

Steel Layer

$$\left[\overline{D_{in}}\right]=\begin{bmatrix} \rho_{si}\bar{E}_{si} & 0 & 0 \\ 0 & 0 & 0 \\ 0 & 0 & 0 \end{bmatrix}$$

$\bar{E}_{si}$ is the uniaxial tangent modulus of embedded in-plane reinforcement

Out-of-plane:

Concrete Layer

$$\left[\overline{D_{out}}\right]=K_s\begin{bmatrix} G_{xz} & 0 \\ 0 & G_{yz} \end{bmatrix}$$

$$G_{xz}=G_{xz}=G_0=E_0/2(1+\nu)$$

K_s shear correction factor, taken as 5/6 **(Maekawa et al. 2003)**

E_0 Elastic modulus of concrete, $3875\sqrt{f_c'(\text{MPa})}$ **(Hsu & Mo, 2010)**

ν Poisson ratio of concrete, taken as 0.2

3. Implementation

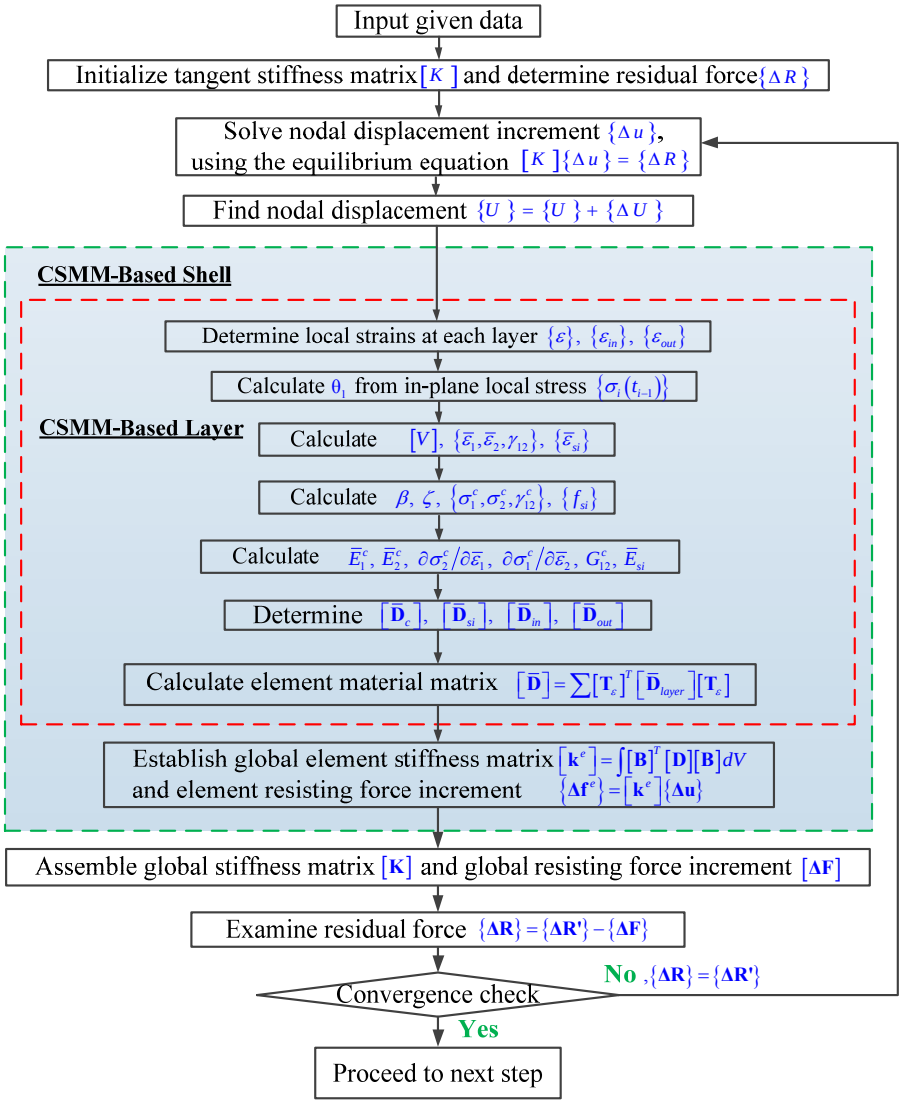

Analysis Procedure

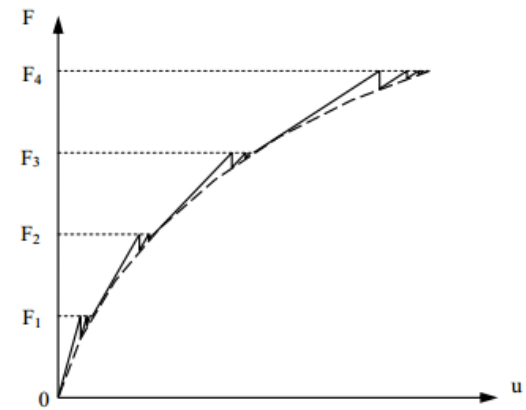

KrylovNewton Method (Carlson & Miller 1998)

Solution Algorithm (OpenSees)

$$\frac{\sqrt{\sum R_i^T R_i}}{\sqrt{\sum R_0^T R_0}} < TOL \qquad \text{For force}$$

$$\frac{\sqrt{\sum (\Delta U_i)^2}}{\sqrt{\sum (\Delta U_0)^2}} < TOL \qquad \text{For displacement}$$

ΔU_i is the nodal displacement increment

R_i is the unbalanced nodal force

TOL is the specified tolerance

Convergence Criterion (OpenSees)

3. Implementation

Development of Finite Element Program SCS-3D

Element and Material Classes of SCS-3D Program

Module	Type	Remark
ConcreteZ01	UniaxialMaterial	Uniaxial constitutive model for concrete **(Zhong, 2005)**
SteelZ01	UniaxialMaterial	Uniaxial constitutive model for steel **(Zhong, 2005)**
CSMMLayer	NDMaterial	3D material model for each layer of CSMM-based shell element
CSMMShellS8	Element	8-node CSMM-based shell element

OpenSees

```
        OpenSees -- Open System For Earthquake Engineering Simulation
      Pacific Earthquake Engineering Research Center -- 2.4.3 (rev 5634)

          (c) Copyright 1999-2013 The Regents of the University of California
                                 All Rights Reserved
    (Copyright and Disclaimer @ http://www.berkeley.edu/OpenSees/copyright.html)


      ***********************************************************************
      *                                                                     *
      *       University of Houston Research Group (OpenSees SCS 3D)        *
      *                                                                     *
      ***********************************************************************

OpenSees > source run.tcl
```

Implementation of element and material classes of SCS-3D program in OpenSees framework

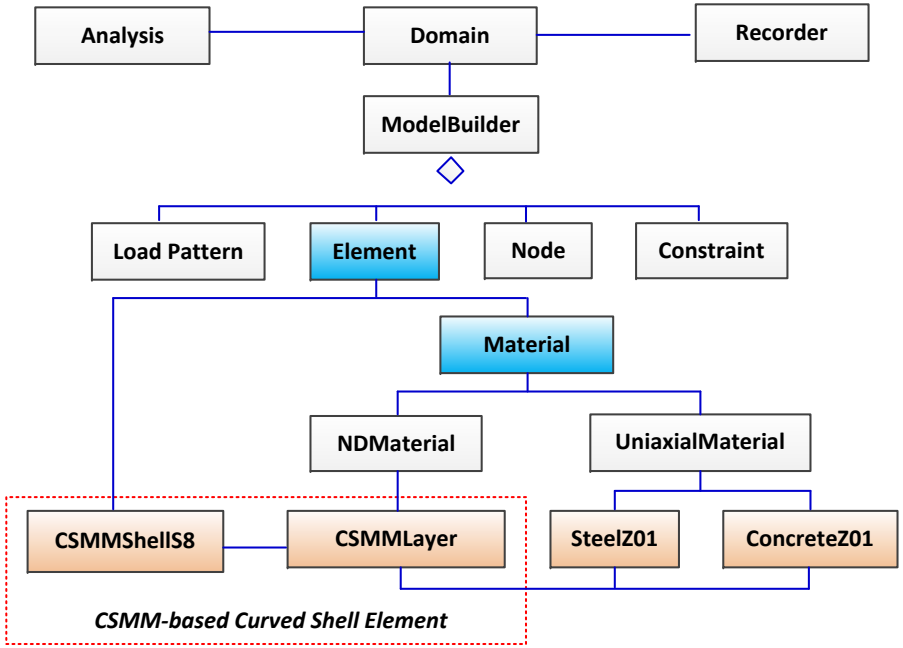

3. Implementation

Development of User Interface for Pre- and Post-Processing using Eyeshot Framework (Cont.)

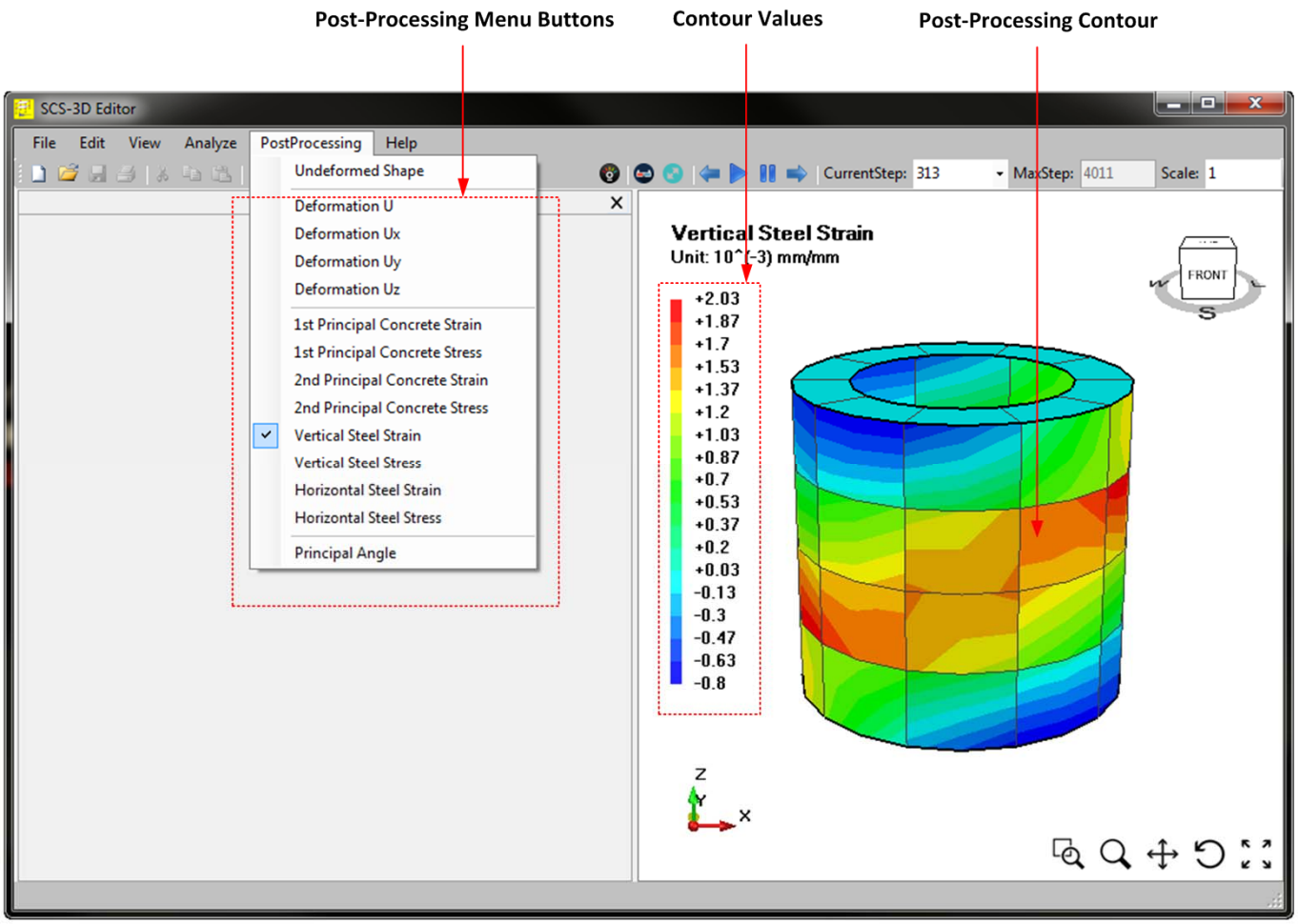

3. Implementation

Sensitivity Analysis

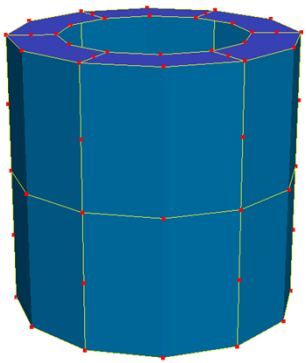

12 Elements

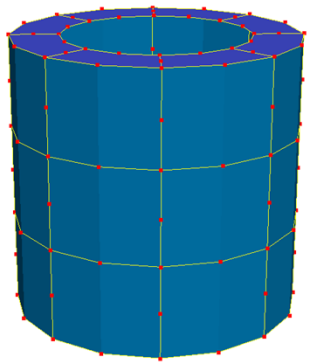

24 Elements

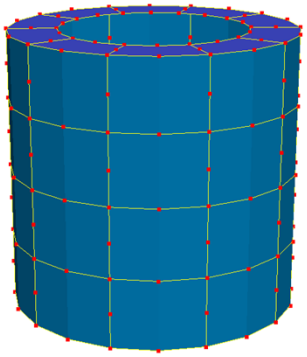

40 Elements

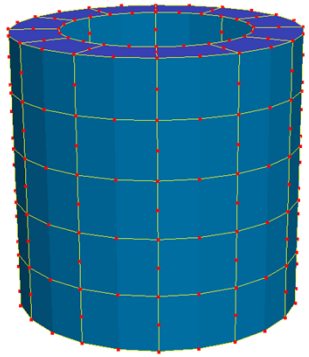

60 Elements

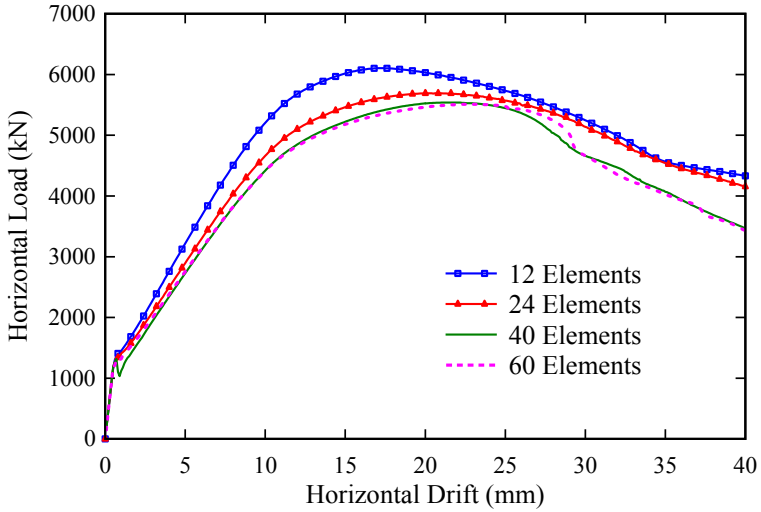

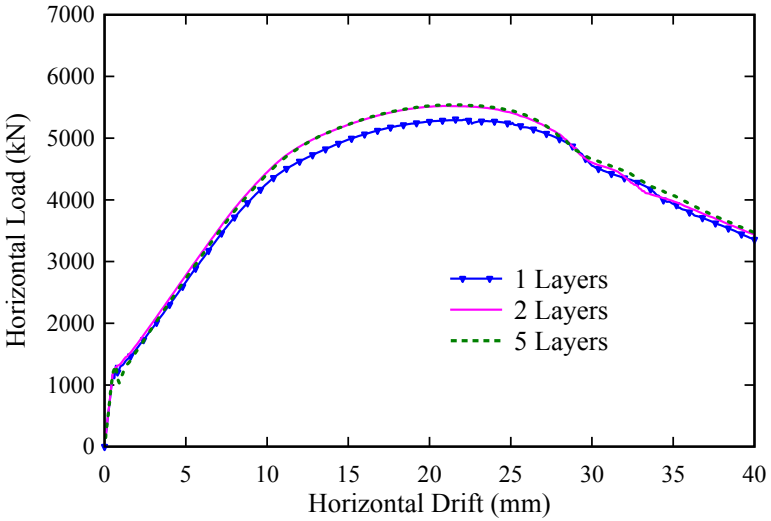

Accurate solution would be achieved even with fewer number of elements or large mesh size of elements.

4. Validations

4. Validations

Element Level

- RC panels under in-plane loadings
- RC panels under in-plane and out-of-plane loadings

Structure Level

- RC Cylindrical Tank
- RC 3D Shear Wall
- RC Hollow Bridge Piers

4. Validations

RC Panels Tested by Pang (1991)

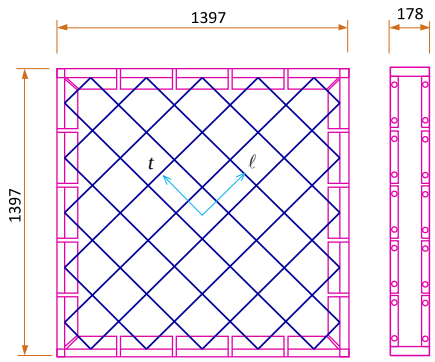

Dimensions of the specimens

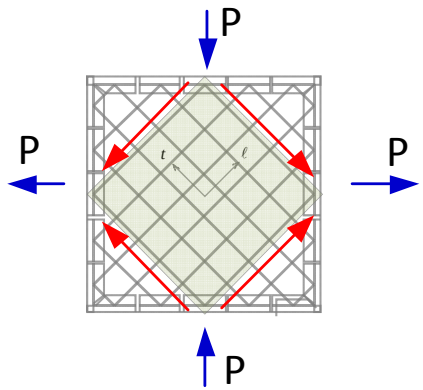

Loading Scheme

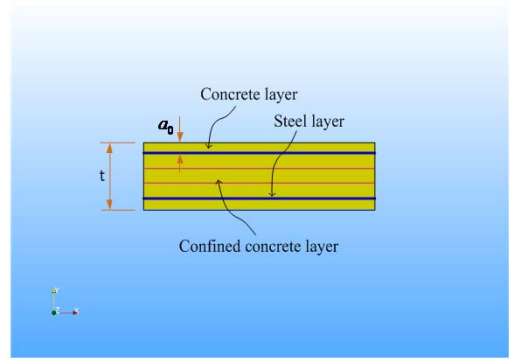

Cross section mesh

Material Properties

Specimen Name	f'_c (MPa)	Reinforcement in ℓ-direction		Reinforcement in t-direction	
		f_y (MPa)	ρ_ℓ (%)	f_y (MPa)	ρ_t (%)
A2	41	463	1.19	463	1.19
A3	42	447	1.79	447	1.79
A4	42	470	2.98	470	2.98

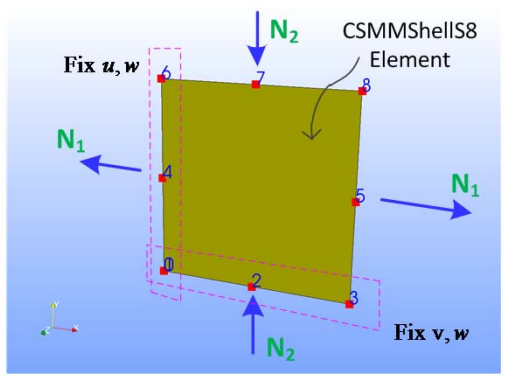

Finite element model

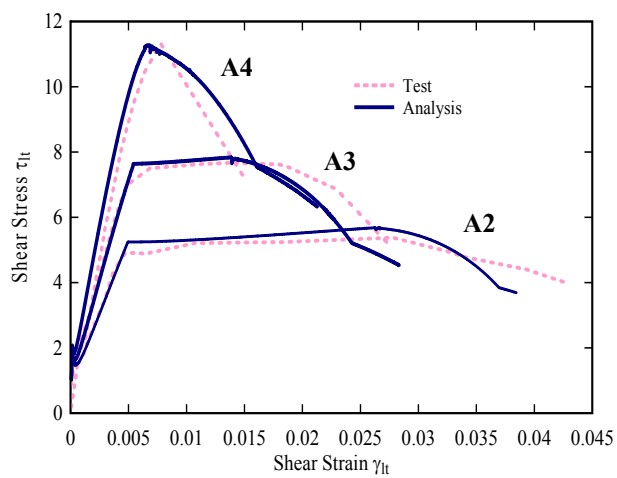

Comparisons of experimental and analytical results

4. Validations

RC Panels Tested by Mansour (2001)

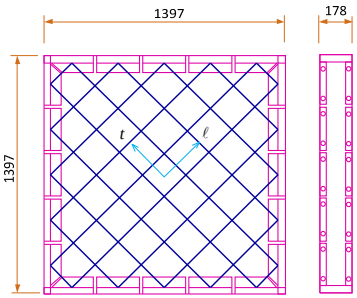

Panel CA3

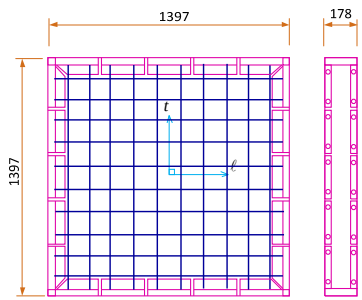

Panel CE4

Dimensions of the specimens

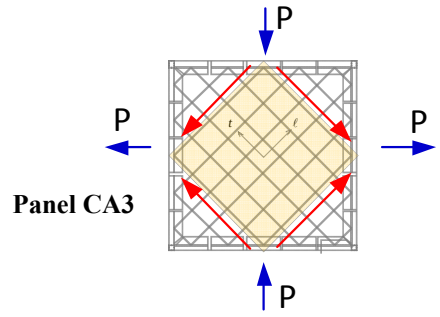

Panel CA3

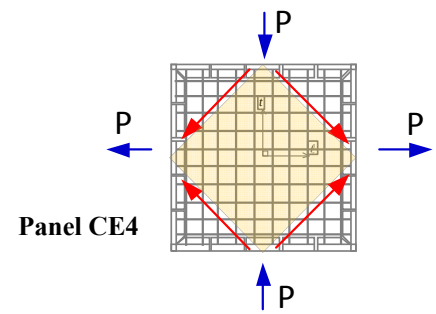

Panel CE4

Loading schemes

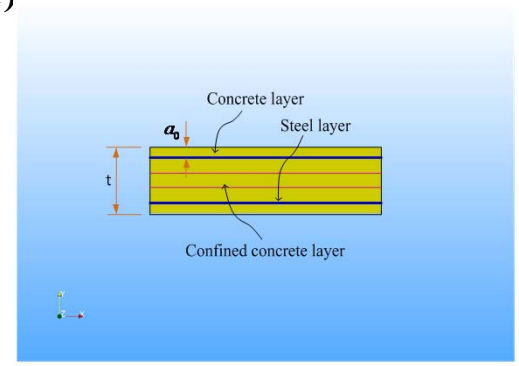

Cross section mesh

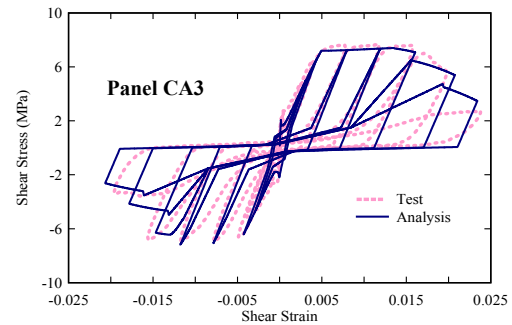

Material Properties

Specimen Name	f'_c (MPa)	Reinforcement in ℓ-direction		Reinforcement in t-direction	
		f_y (MPa)	ρ_ℓ (%)	f_y (MPa)	ρ_t (%)
CA3	46	425.4	1.7	425.4	1.7
CE3	48	453.4	1.9	453.4	1.9

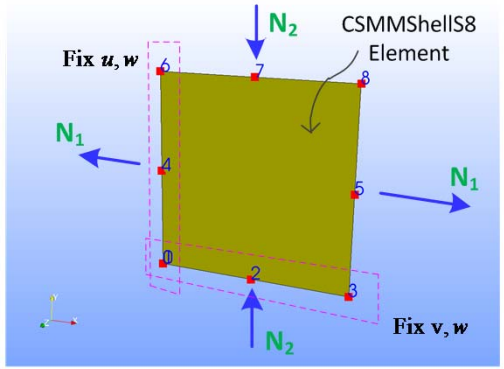

Finite element model

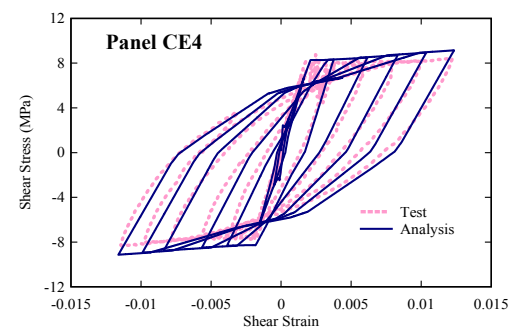

Comparisons of experimental and analytical results

4. Validations

RC Panels Tested by Polak (1992)

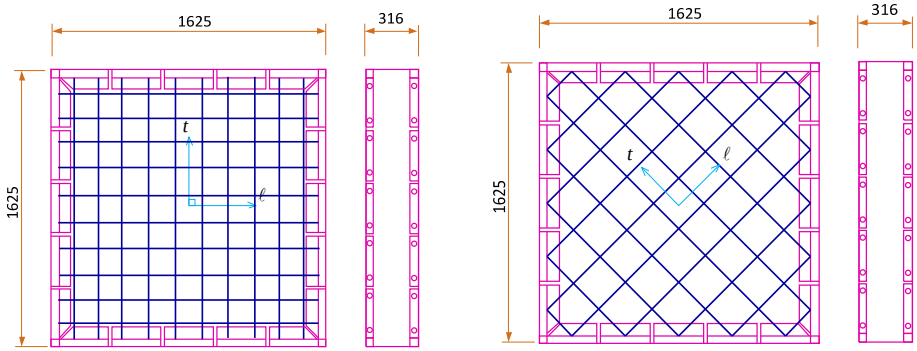

Dimensions of the specimens

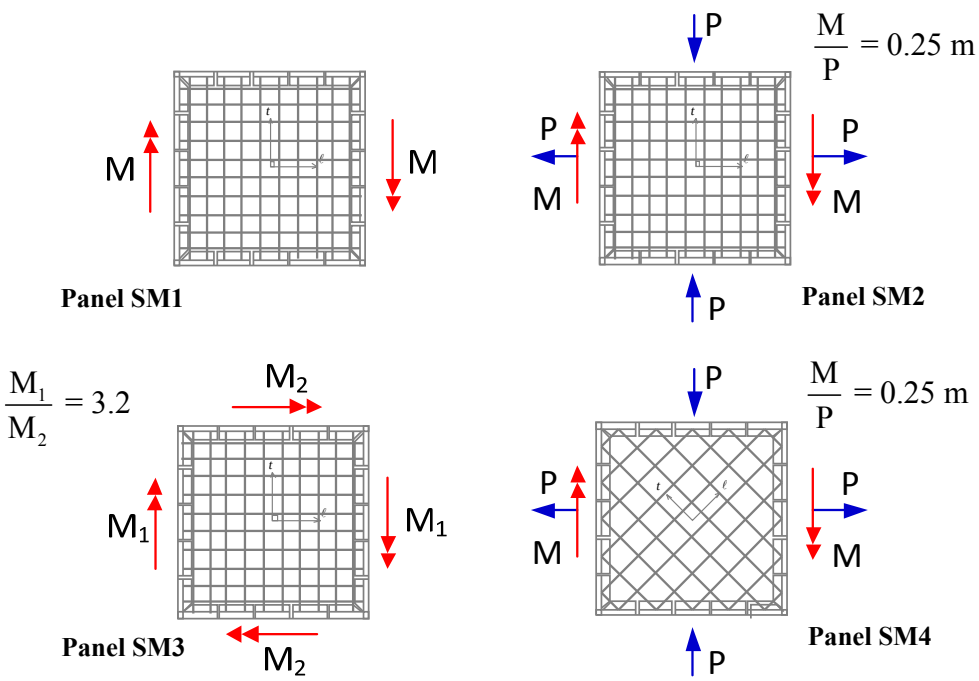

Loading scheme

Loading and Material Properties

Specimen Name	f'_c (MPa)	Reinforcement in x-direction		Reinforcement in y-direction	
		f_y (MPa)	ρ_x^* (%)	f_y (MPa)	ρ_y^* (%)
SM1	47	425	1.25	430	0.42
SM2	62	425	1.25	430	0.42
SM3	56	425	1.25	430	0.42
SM4	64	425	1.25	430	0.42

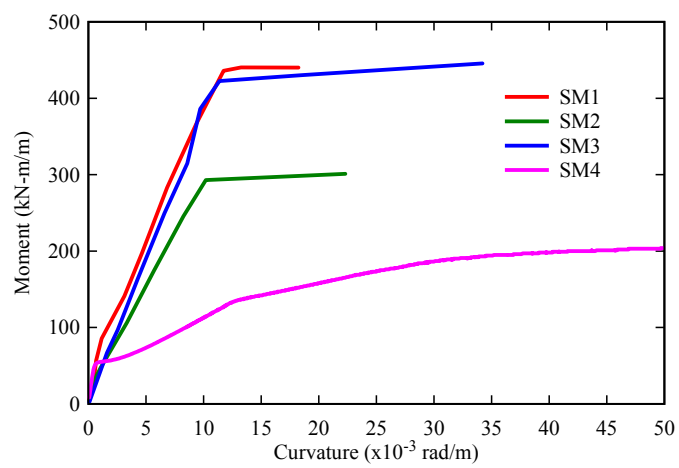

Experimental results

4. Validations

RC Panels Tested by Polak (1992) (Cont.)

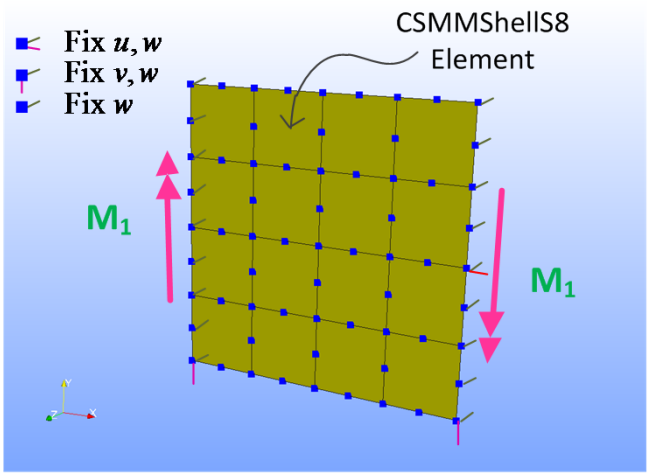

Finite element model (Panel SM1)

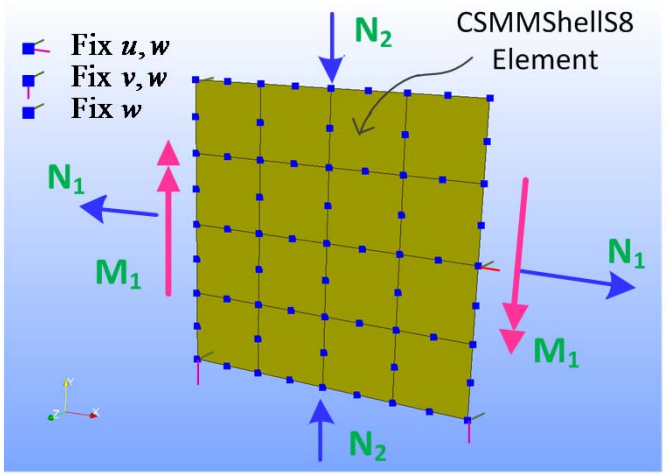

Finite element model (Panel SM2 and SM4)

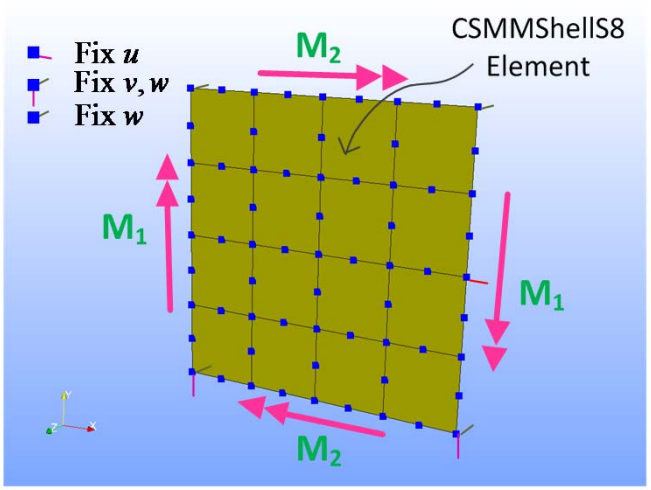

Finite element model (Panel SM3)

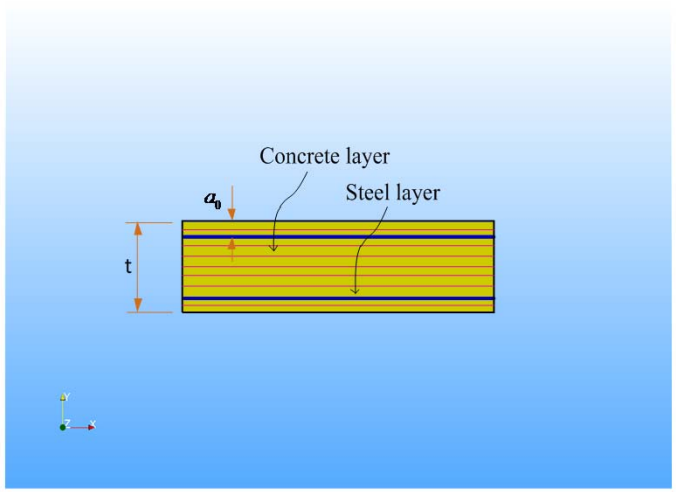

Cross section mesh

4. Validations

RC Panels Tested by Polak (1992) (Cont.)

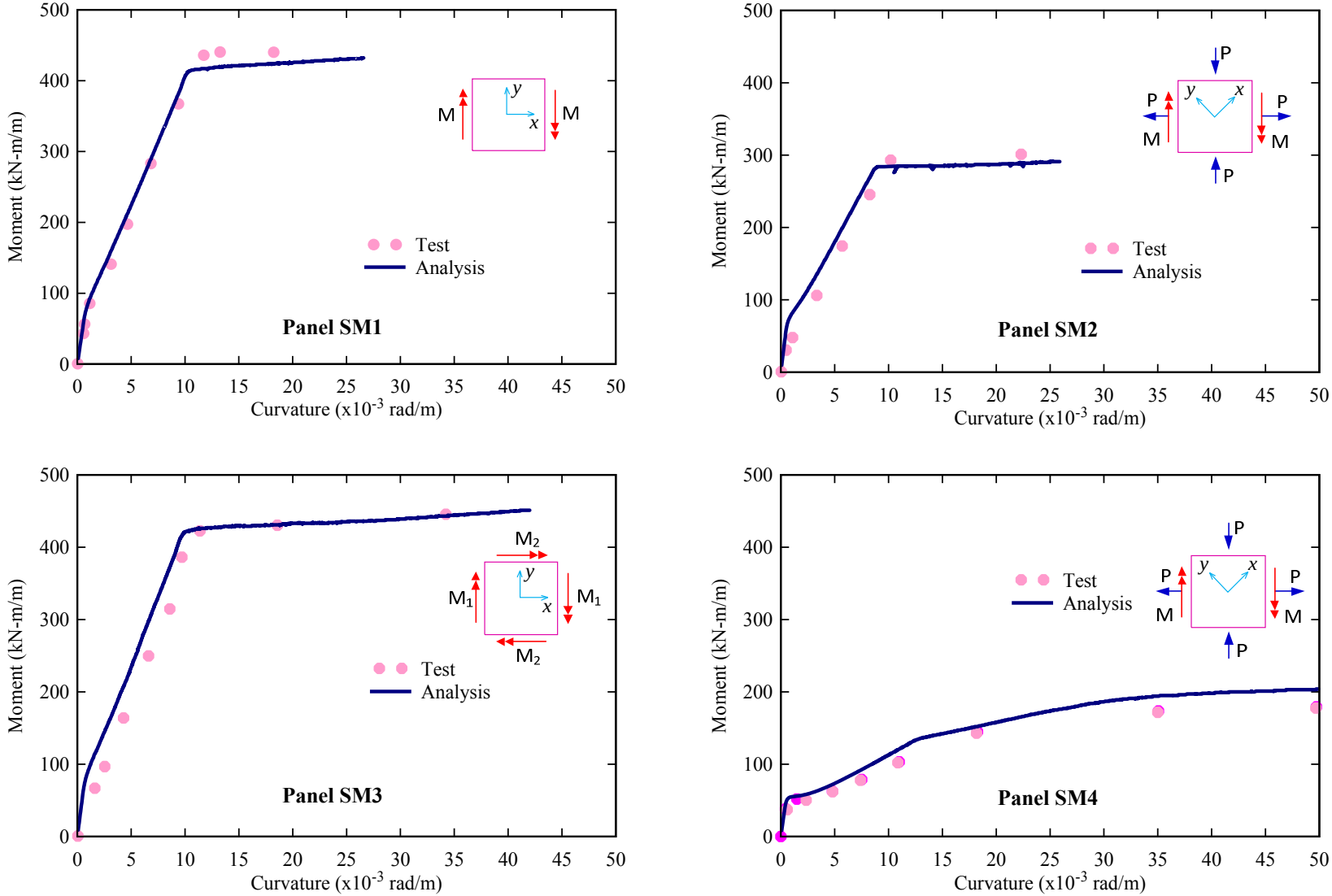

Comparisons of experimental and analytical results

4. Validations

RC Cylindrical Tank (Maekawa et al., 2003)

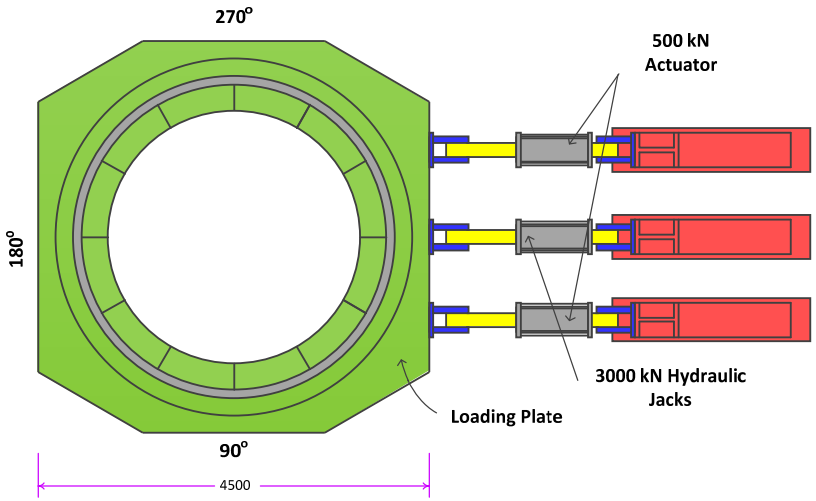

Test Setup (Plan view)

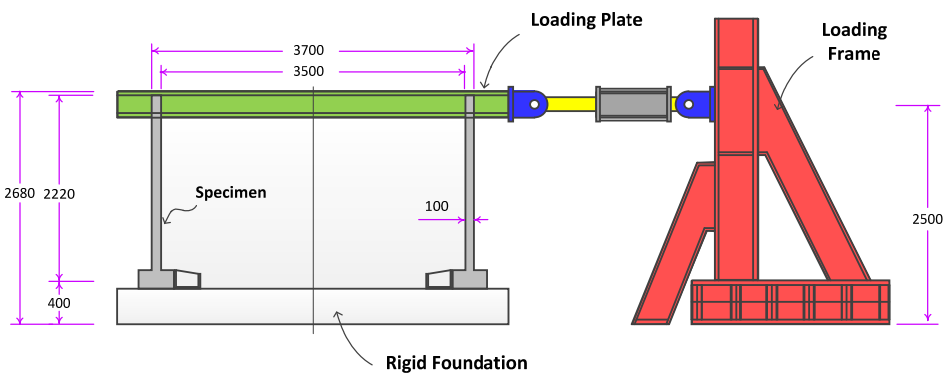

Test Setup (Elevation view)

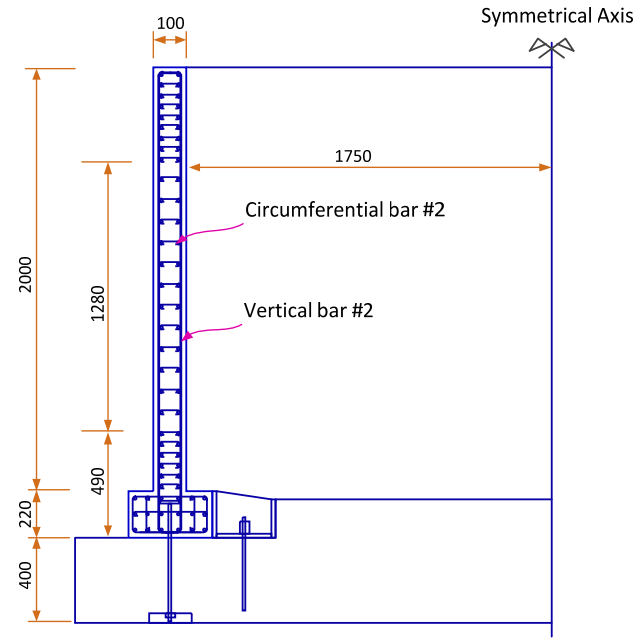

Dimension and reinforcement detailing of the specimen

Dimension and material properties

Specimen	f'_c (MPa)	D (mm)	H (mm)	t (mm)	Vertical Reinforcement		Horizontal Reinforcement	
					f_y (MPa)	ρ_v (%)	f_y (MPa)	ρ_h (%)
1	28.0	3600	2000	100	384.0	0.8	410.0	0.8

Note : f'_c = Compressive strength of concrete; D = Diameter of the tank; t = Thickness f_y = Yielding strength of steel; H = Effective height of the tank; ρ_v = Percentage of the vertical steel; ρ_h = Percentage of horizontal steel.

4. Validations

RC Cylindrical Tank (Maekawa et al., 2003) (Cont.)

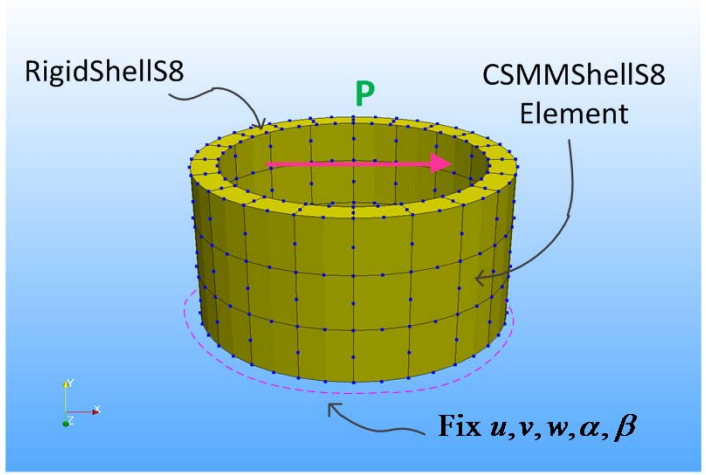

Finite element model

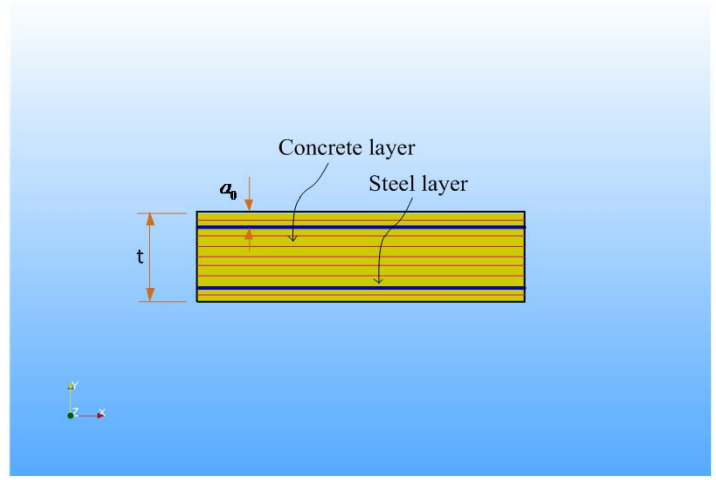

Cross section mesh

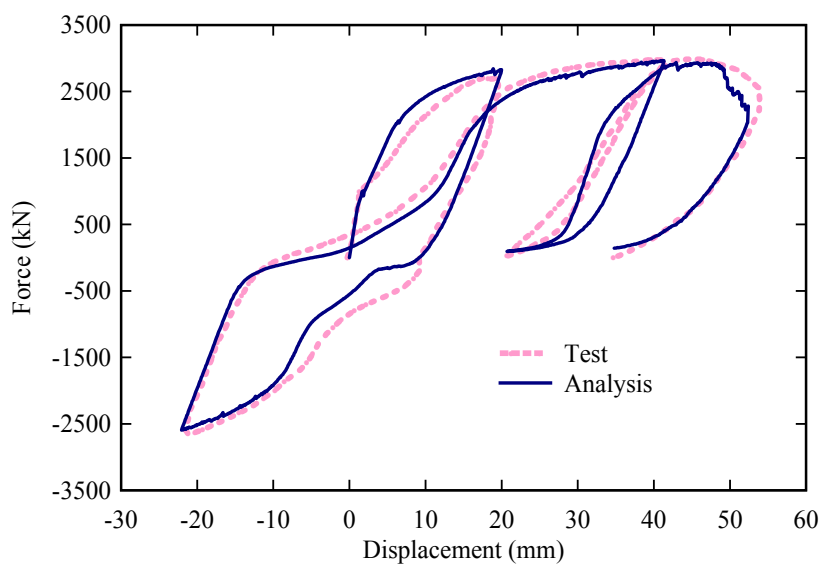

Comparison of experimental and analytical results

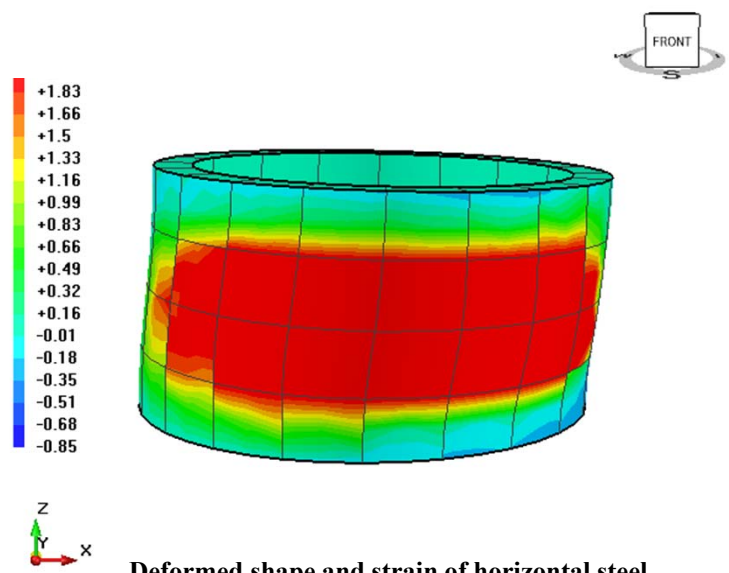

Deformed shape and strain of horizontal steel bars at the peak load

4. Validations

3D RC Shear Wall (Palermo and Vecchio, 2002)

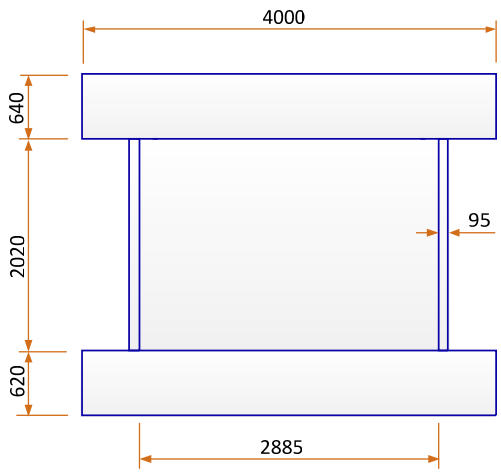

Dimension of the specimen

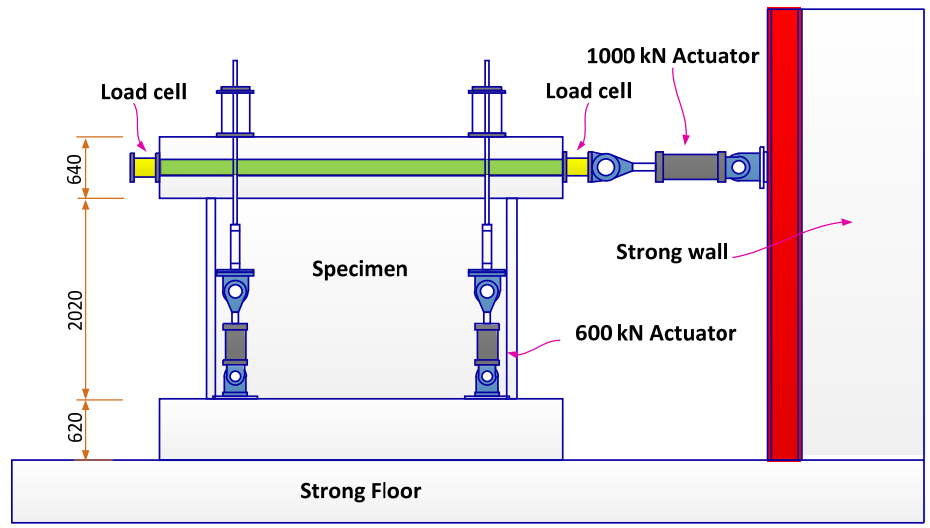

Test Setup (Elevation view)

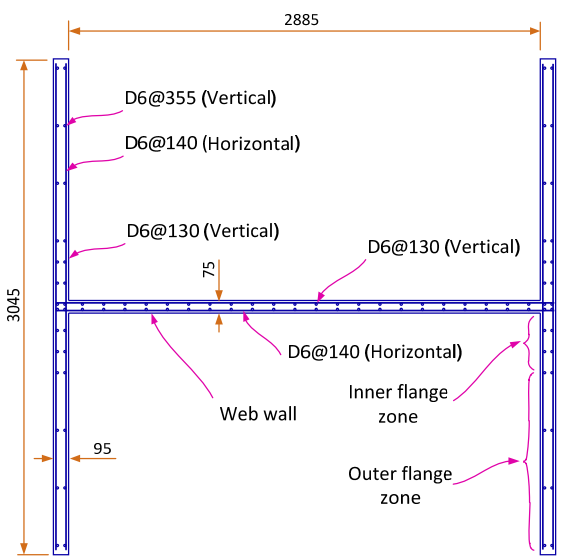

Reinforcement detailing of the specimen

Dimension and material properties

Wall Zone	f'_c (MPa)	P (kN)	$\frac{P}{f'_c A_g}$	L (mm)	Longitudinal Reinforcement		Transverse Reinforcement	
					f_y (MPa)	ρ_l (%)	f_y (MPa)	ρ_s (%)
Web	21.7	940	0.054	2020	605.0	0.8	605.0	0.73
Inner Flange						0.62		0.58
Outer Flange						0.23		0.58

Note : f'_c = Compressive strength of concrete; A_g = Area of cross section;
f_y = Yielding strength of steel; L = Effective height of the wall;
ρ_l = Percentage of the longitudinal steel; ρ_s = Percentage of transverse steel.

4. Validations

3D RC Shear Wall (Palermo and Vecchio, 2002) (Cont.)

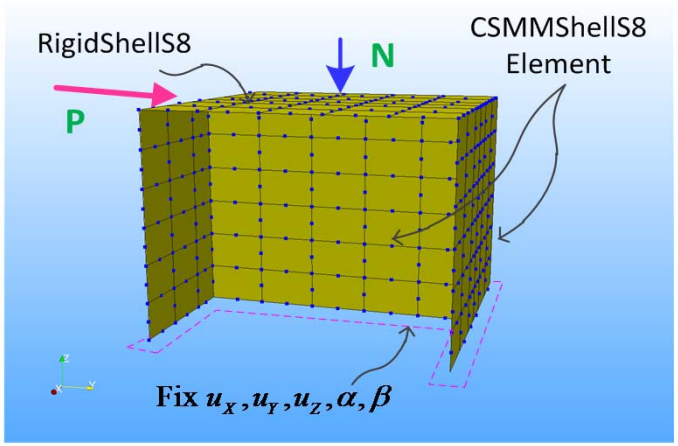

Finite element model

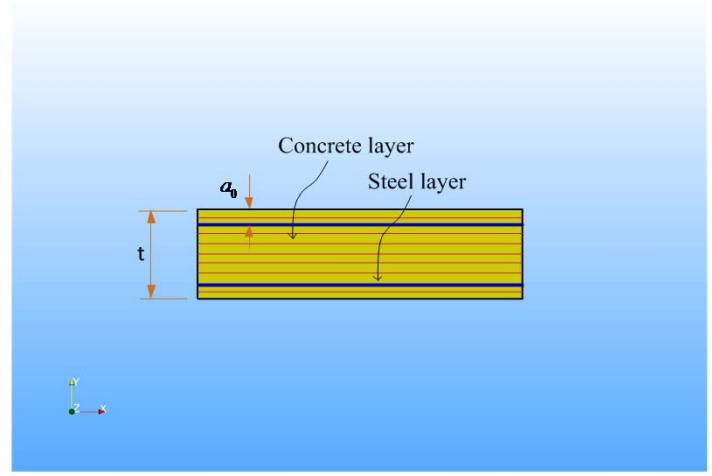

Cross section mesh

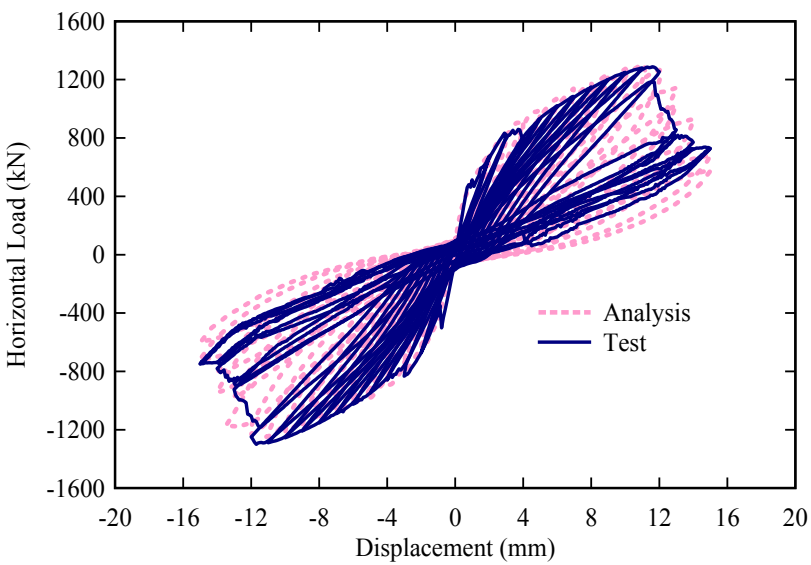

Comparison of experimental and analytical results

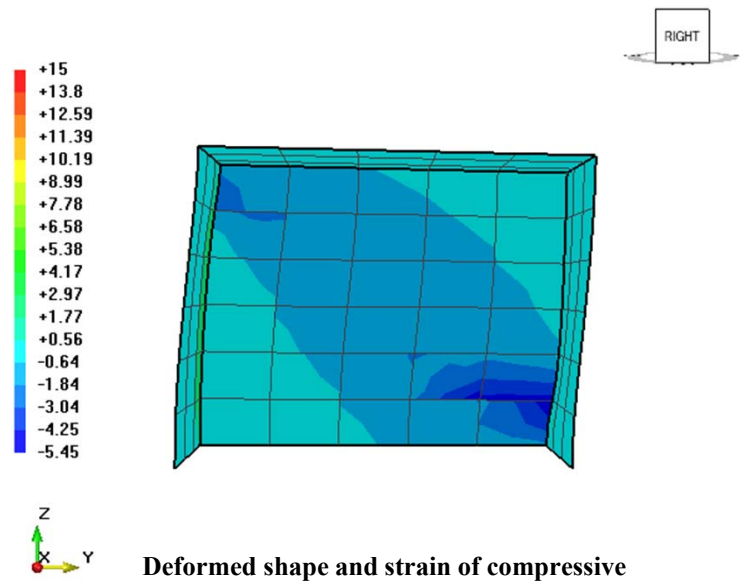

Deformed shape and strain of compressive principal strain of concrete at the peak load

4. Validations

RC Hollow Bridge Piers (Yeh & Mo, 1999; 2001)

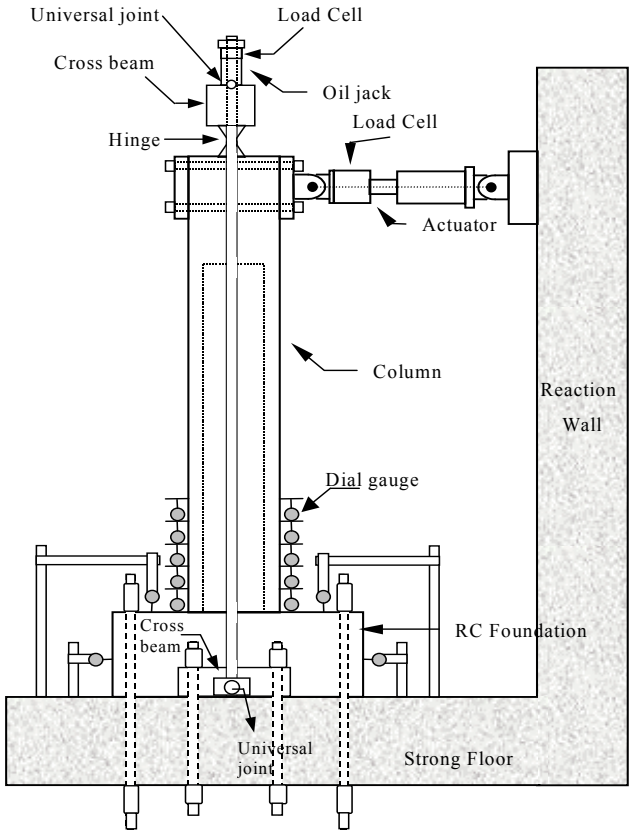

Test Setup (Elevation view)

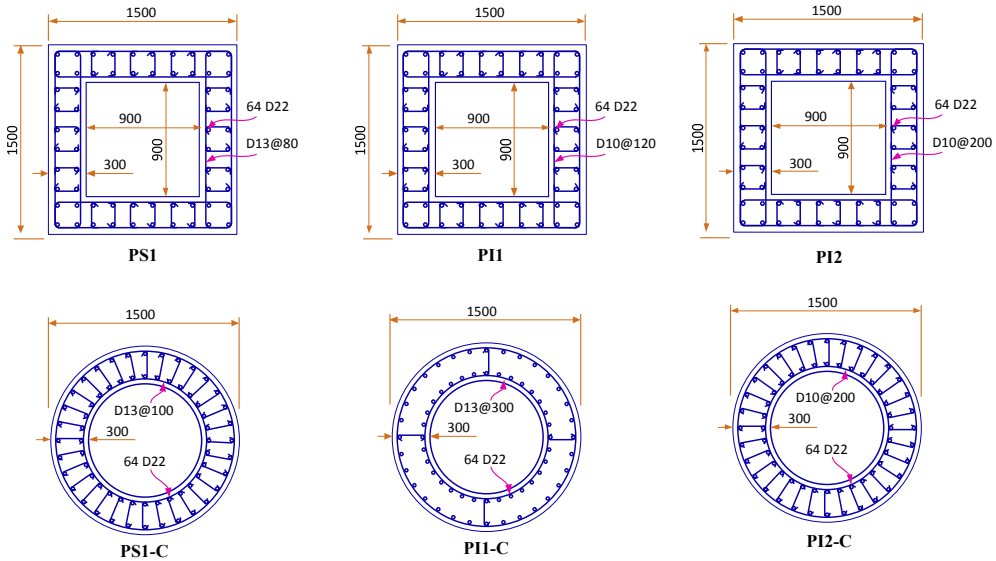

Cross-section of the specimens

Material Properties

Specimen Name	f'_c (MPa)	P (kN)	$\frac{P}{f'_c A_g}$	L (mm)	Longitudinal Reinforcement		Transverse Reinforcement	
					f_y (MPa)	ρ_l (%)	f_y (MPa)	ρ_s (%)
PS1	34.0	4000	0.082	6500	460.0	1.7	343.0	1.1
PI1	34.0	4000	0.082	4500	460.0	1.7	510.0	0.45
PI2	32.0	3600	0.078	3500	418.2	1.7	420.0	0.26
PS1-C	31.7	3600	0.101	5500	418.2	2.15	410.0	0.9
PI1-C	33.8	3600	0.094	5500	418.2	2.15	410.0	0.3
PI2-C	30.9	3600	0.103	3500	418.2	2.15	410.0	0.26

Note : f'_c = Compressive strength of concrete; A_g = Area of cross section;
f_y = Yielding strength of steel; L = Effective height of the column;
ρ_l = Percentage of the longitudinal steel; ρ_s = Percentage of transverse steel.

4. Validations

RC Hollow Bridge Piers (Yeh & Mo, 1999; 2001) (Cont.)

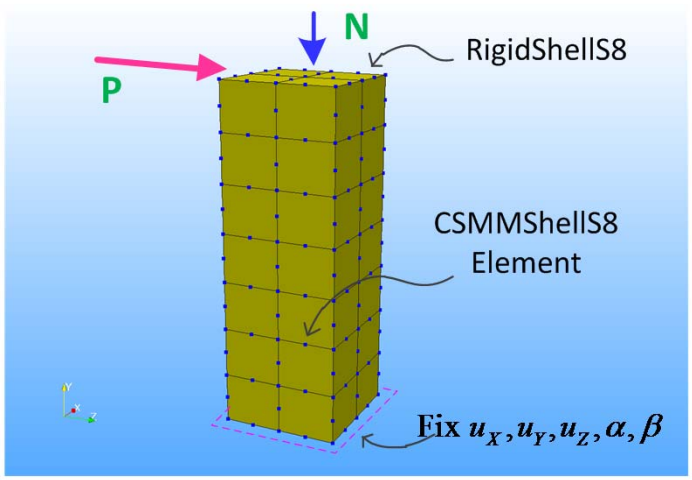

Finite element model for the specimens PS1, PI1, PI2

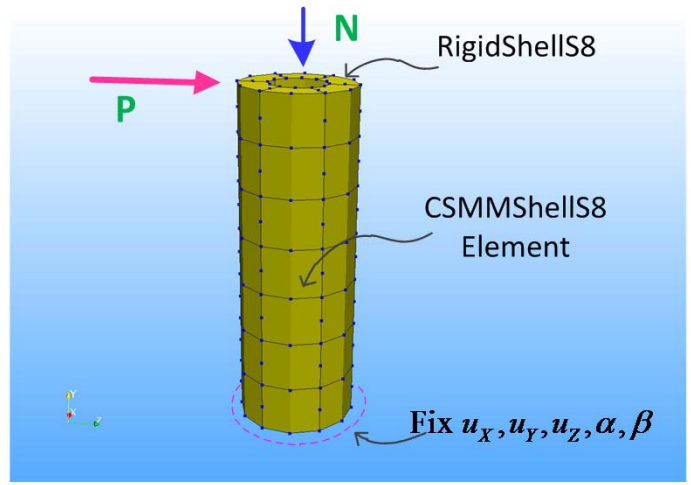

Finite element model for the specimens PS1-C, PI1-C, PI2-C

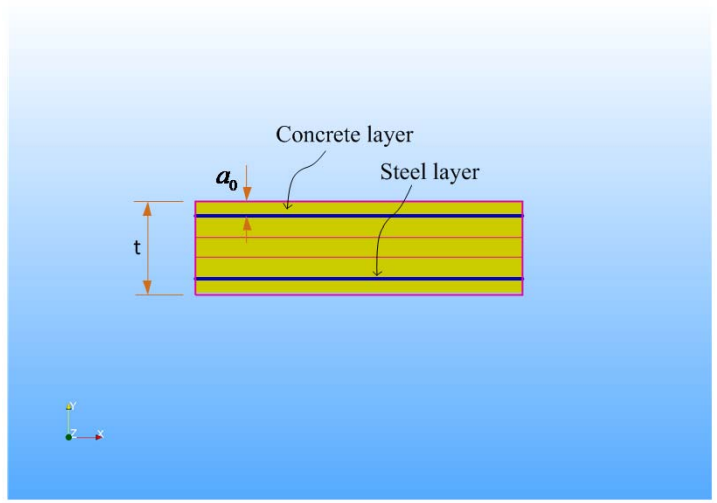

Cross section mesh

4. Validations

RC Hollow Bridge Piers (Yeh & Mo, 1999; 2001) (Cont.)

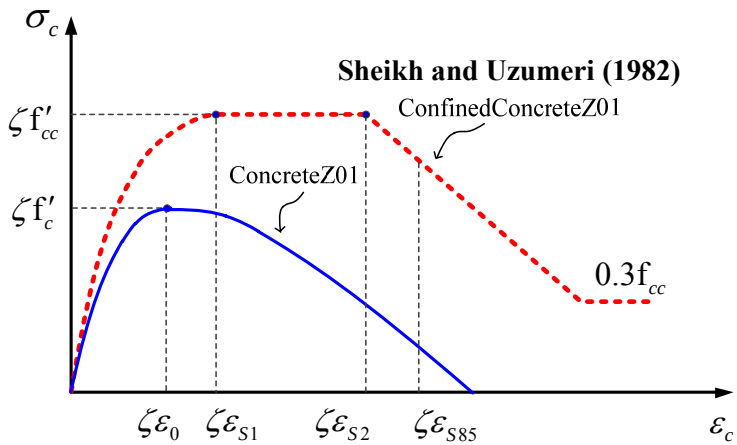

The confined concrete model for CSMM

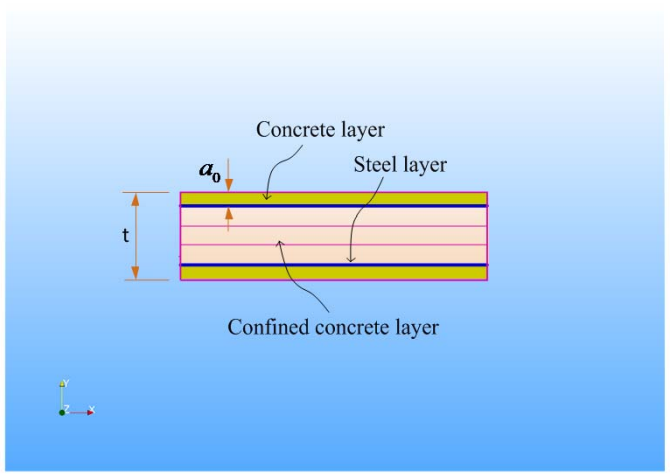

Cross section mesh considering confinement effect

Summary of equations for the confined concrete model:

$$\sigma_c = D\zeta f'_{cc}\left[2\left(\frac{\bar{\varepsilon}}{\zeta\varepsilon_{01}}\right)-\left(\frac{\bar{\varepsilon}}{\zeta\varepsilon_{01}}\right)^2\right], \qquad 0\le|\bar{\varepsilon}|\le|\zeta\varepsilon_{01}|,$$

$$\sigma_c = D\zeta f'_{cc}, \qquad |\zeta\varepsilon_{01}|\le|\bar{\varepsilon}|\le|\zeta\varepsilon_{02}|,$$

$$\sigma_c = D\zeta f'_{cc}\left[1-Z\left(\bar{\varepsilon}-\varepsilon_{02}\right)\right]\ge 0.3D\zeta f'_{cc}, \qquad |\bar{\varepsilon}|>|\zeta\varepsilon_{02}|,$$

$$f'_{cc} = K_s f'_c,$$

$$K_s = 1.0+\frac{A_{co}}{140P_{occ}}\left[\left(1-\frac{nc^2}{5.5A_{co}}\right)\left(1-\frac{s}{2B}\right)\right]\sqrt{\rho_s f_{yh}},$$

$$P_{occ} = 0.85f'_c\left(A_{co}-A_s\right),$$

$$\varepsilon_{S1} = 80\times10^{-6}\cdot K_s\cdot f'_c,$$

$$\varepsilon_{S2} = 0.0022\left[1+\frac{248}{c}\left(1-5\left(\frac{s}{B}\right)^2\right)\frac{\rho_s f_{yh}}{\sqrt{f'_c}}\right],$$

$$\varepsilon_{85} = 0.225\rho_s\sqrt{\frac{B}{s}}+\varepsilon_{02},$$

$$Z = \frac{0.15}{\varepsilon_{85}-\varepsilon_{02}},$$

4. Validations

RC Hollow Bridge Piers (Yeh & Mo, 1999; 2001) (Cont.)

Comparison between analytical results using confined and confined concrete models

Specimen PS1-C

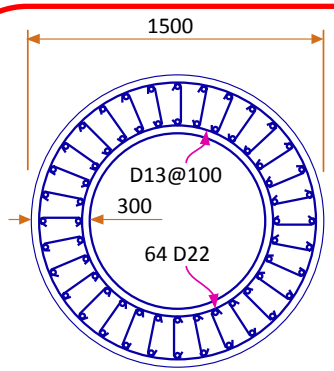

Cross-section of the specimen

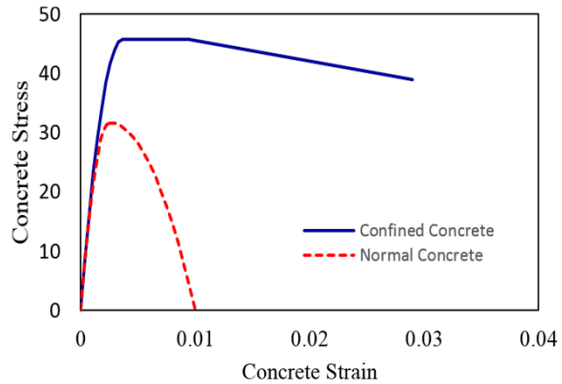

Input compressive stress-strain relationships

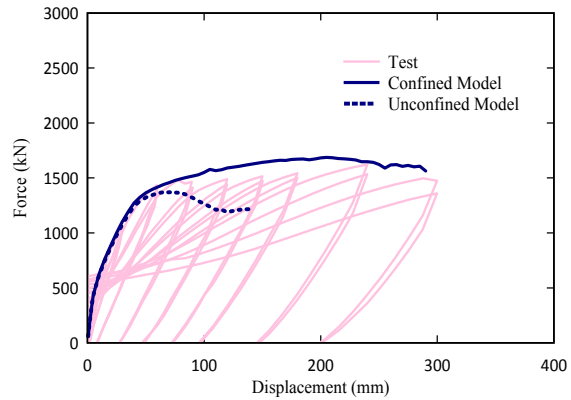

Comparison of analytical results with test result

Specimen PI2-C

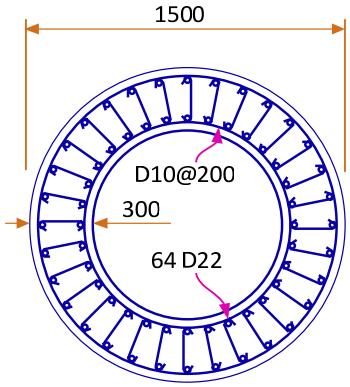

Cross-section of the specimen

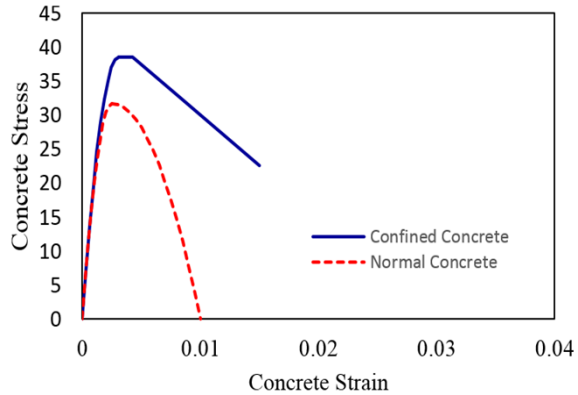

Input compressive stress-strain relationships

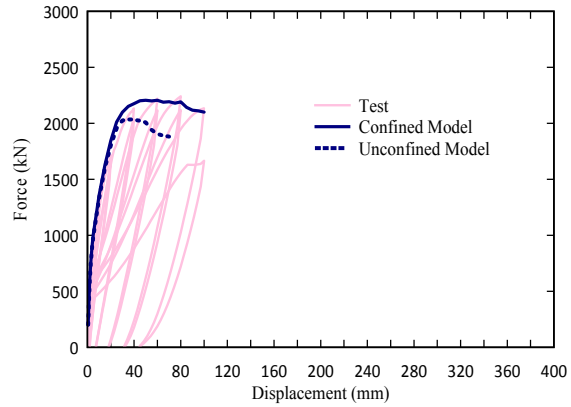

Comparison of analytical results with test result

4. Validations

RC Hollow Bridge Piers (Yeh & Mo, 1999; 2001) (Cont.)

Comparisons of analytical and experimental results using confined model

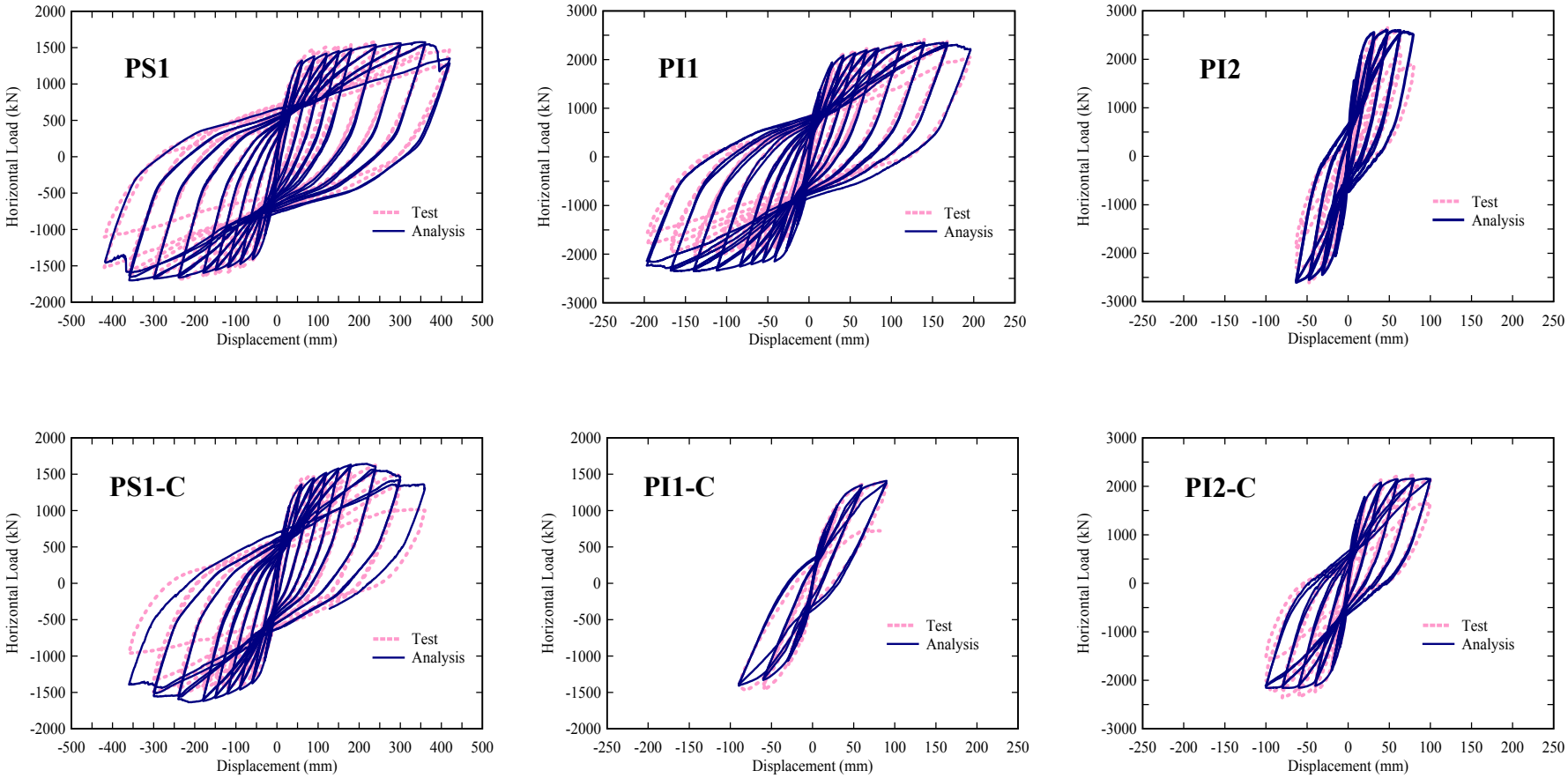

5. Nuclear Containment Vessels

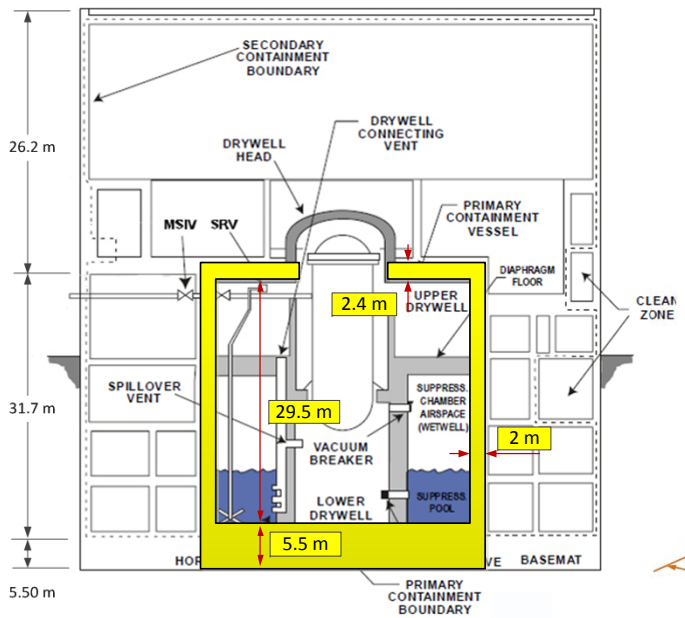

Elevation view

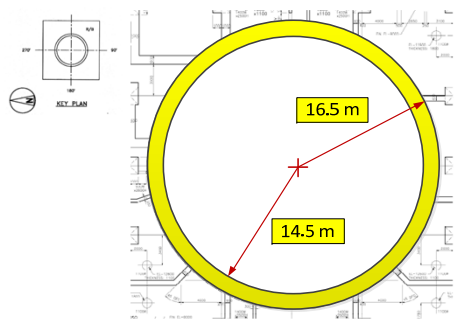

Plan view

Prototype of Lungmen containment vessel

1/13 Scale

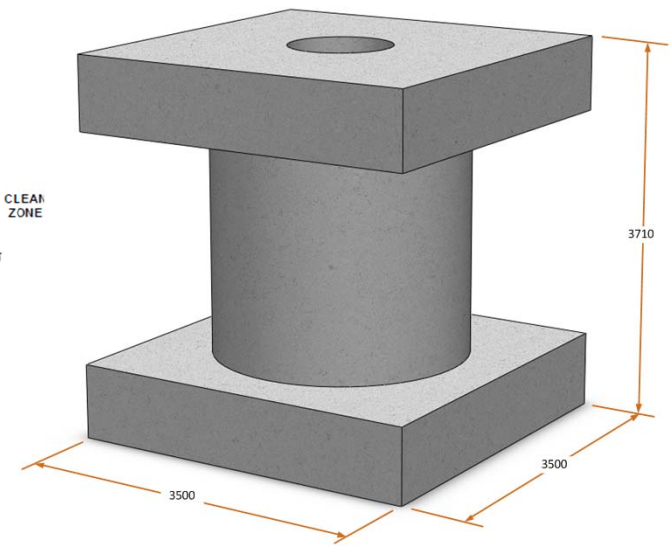

3D view of RCCV specimens

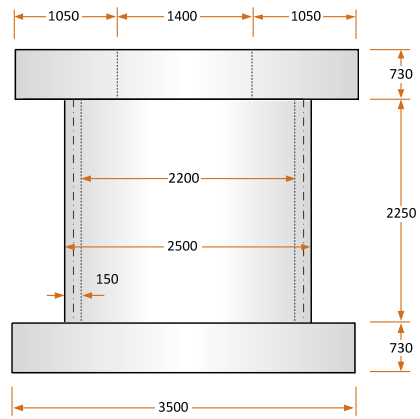

Elevation view

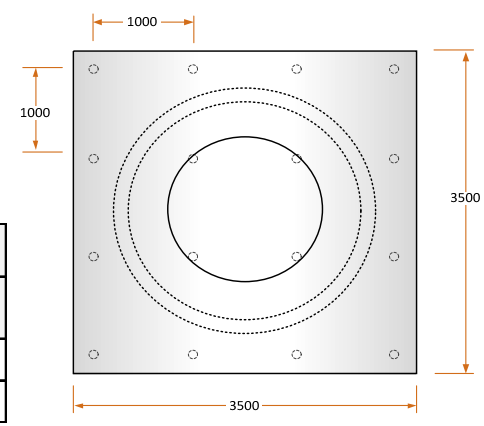

Plan view

Dimensions of RCCV specimens

Specimen No.	f_c' (MPa)	D (mm)	H (mm)	t (mm)	Vertical Reinforcement			Horizontal Reinforcement		
					d_b (mm)	f_y (MPa)	ρ_v (%)	d_b (mm)	f_y (MPa)	ρ_h (%)
RCCV #1	35	2350	2250	150	9.5	365	2	9.5	365	2
RCCV #2	37	2350	2250	150	9.5	365	2 (4)	9.5	365	2

Note : f_c' = Compressive strength of concrete; D = Diameter; H = Net height; t = Thickness; f_y = Yielding strength of steel; d_b = Diameter of steel bar; ρ_v = Steel ratio in the vertical direction; ρ_h = Steel ratio in horizontal direction

5. Nuclear Containment Vessels

Reinforcement Detailing

Specimen No. 1

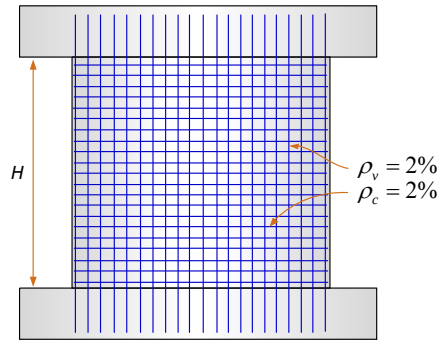

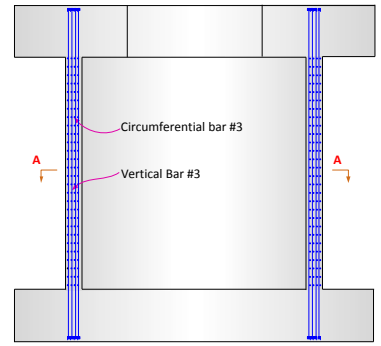

Vertical cross-section

Specimen No. 2

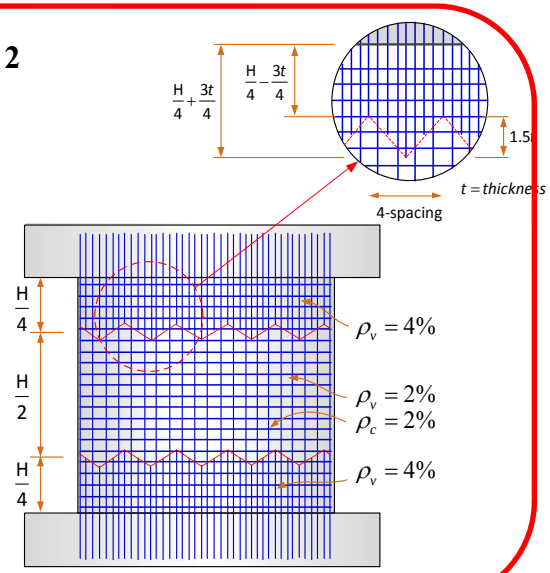

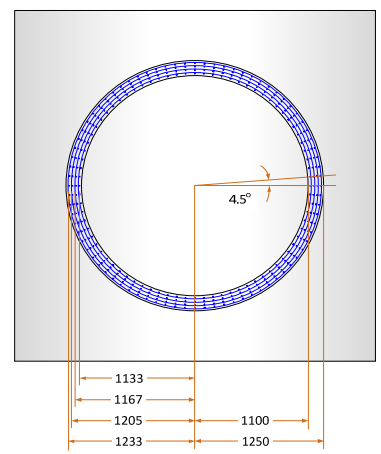

Horizontal cross-section

5. Nuclear Containment Vessels

Manufacturing of Specimens

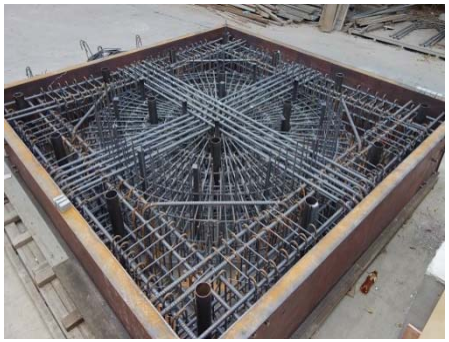

1

2

3

4

5

6

7

8

5. Nuclear Containment Vessels

Strain Gauge Distributions

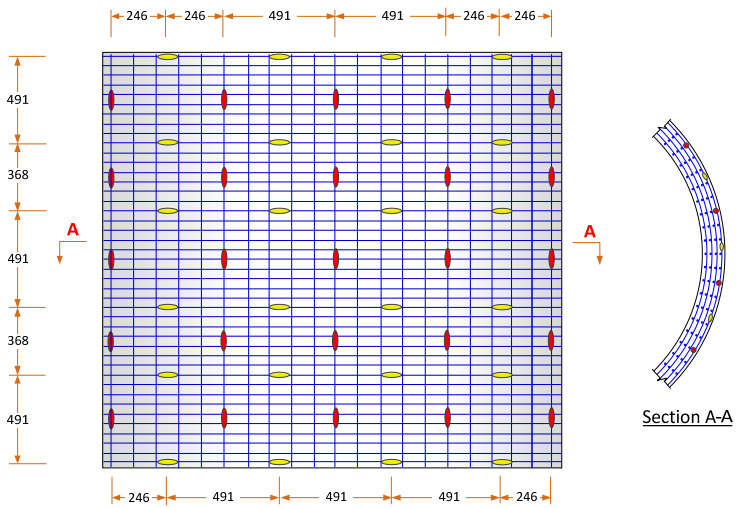

Specimen No. 1

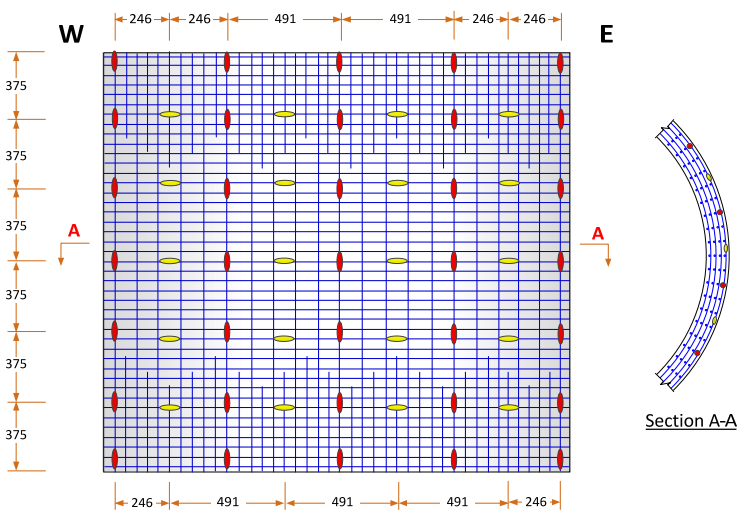

Specimen No. 2

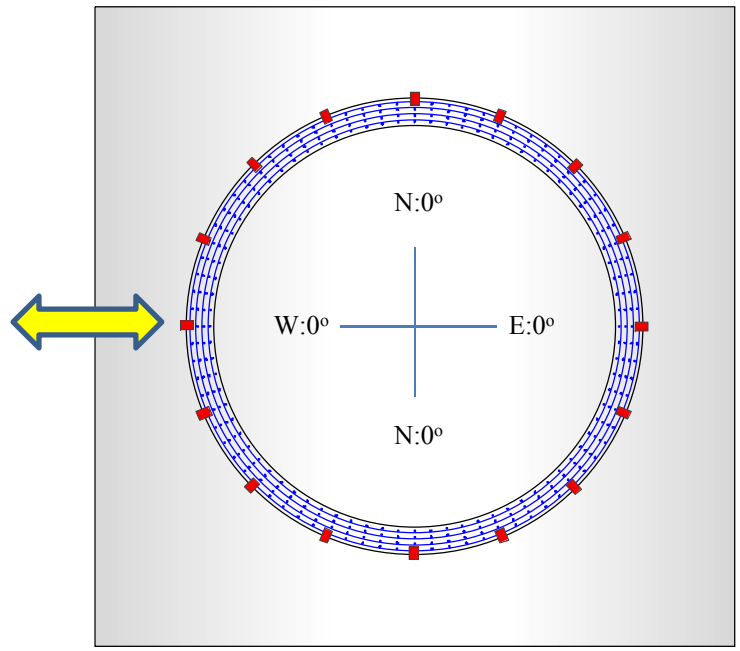

Plan view of strain gauge distribution

5. Nuclear Containment Vessels

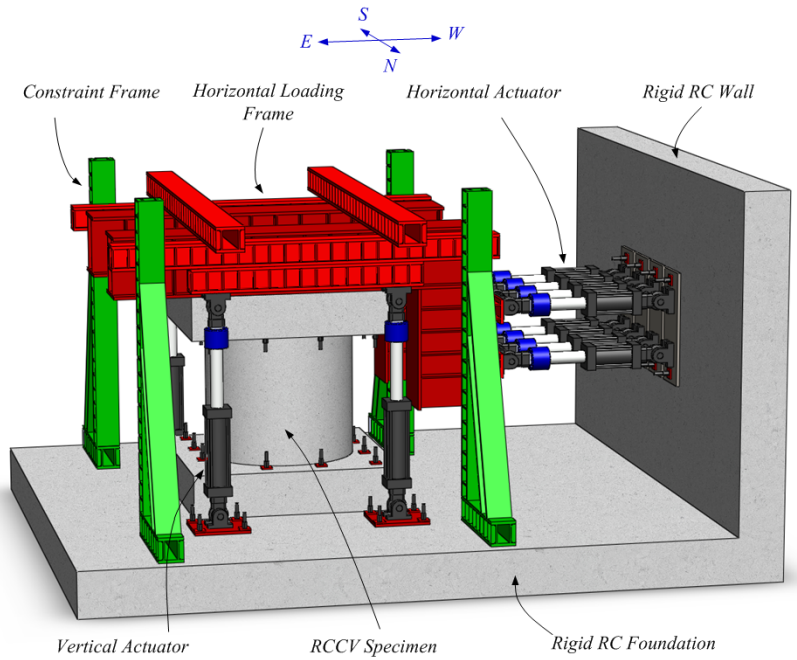

Test setup

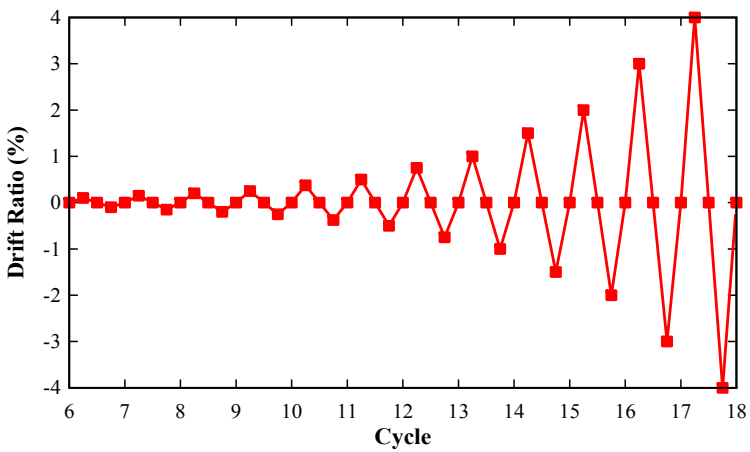

Loading protocol

Testing plan view

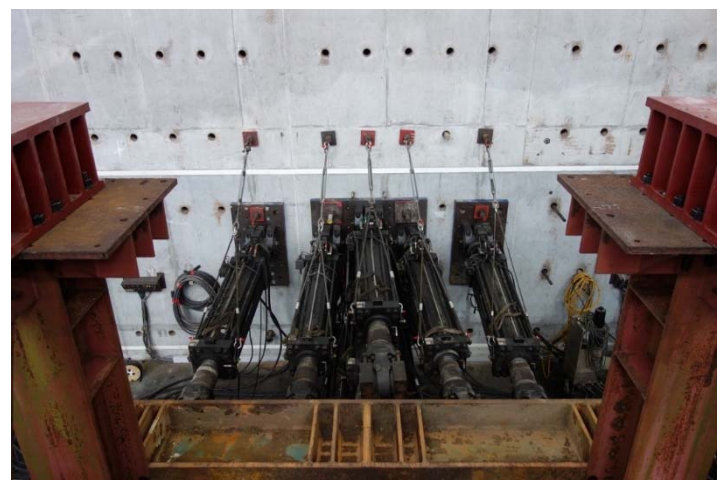

Horizontal actuators (Total: 8000 kN)

5. Nuclear Containment Vessels

Experimental Results

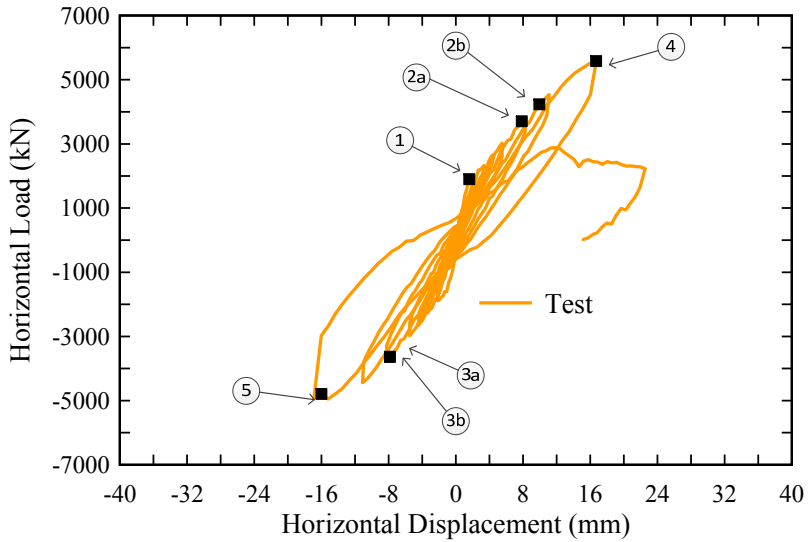

Horizontal load versus displacement curve of Specimen No. 1

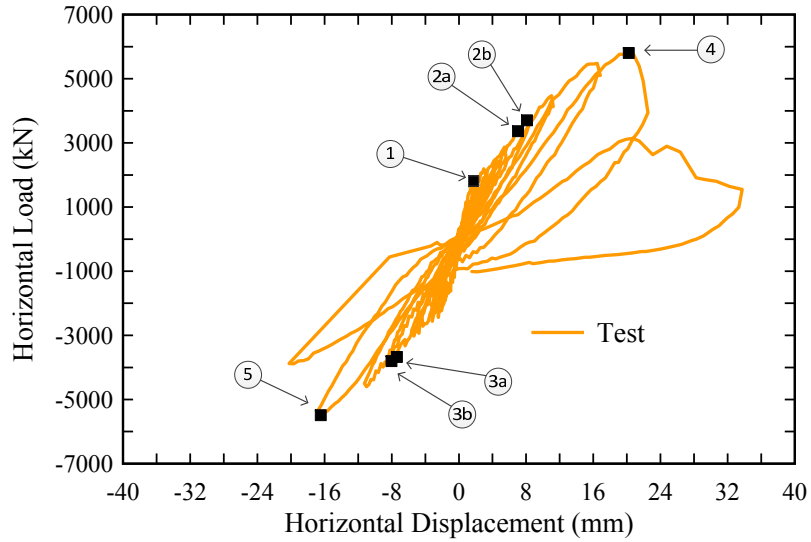

Horizontal load versus displacement curve of Specimen No. 2

Critical Points on the load vs. displacement curves

Points	Status
1	First cracking of concrete
2a	First yield of vertical steel bars in the positive direction
2b	First yield of horizontal steel bars in the positive direction
3a	First yield of vertical steel bars in the negative direction
3b	First yield of horizontal steel bars in the negative direction
4	Peak load in the positive direction
5	Peak load in the negative direction

Experimental Results

Specimen	Loading Direction	Δ_y (mm)	P_y (kN)	Δ_{max} (mm)	P_{max} (kN)	μ
1	(+)	7.84	3706	16.7	5580	2.13
	(-)	7.86	3634	16.0	4794	2.04
2	(+)	7.04	3363	20.2	5805	2.87
	(-)	7.38	3675	16.5	5487	2.23

5. Nuclear Containment Vessels

Failure Mode of Specimen No. 1

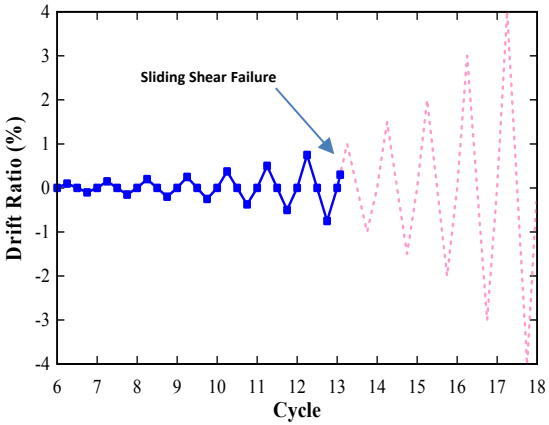

Loading history

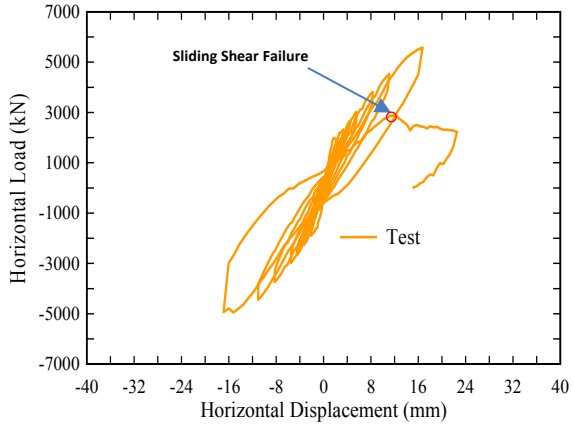

Horizontal load vs. displacement curve

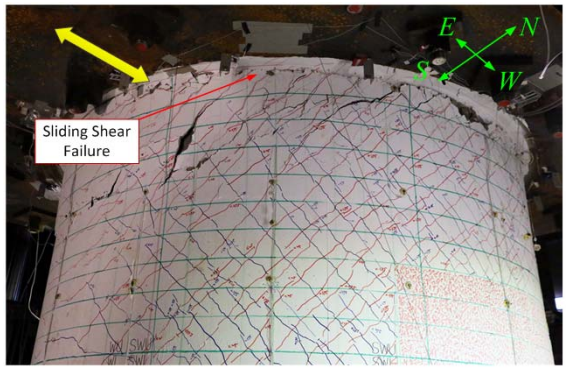

Sliding shear failure
(Cycle 13 – Drift 0.3%)

Failure Mode of Specimen No. 2

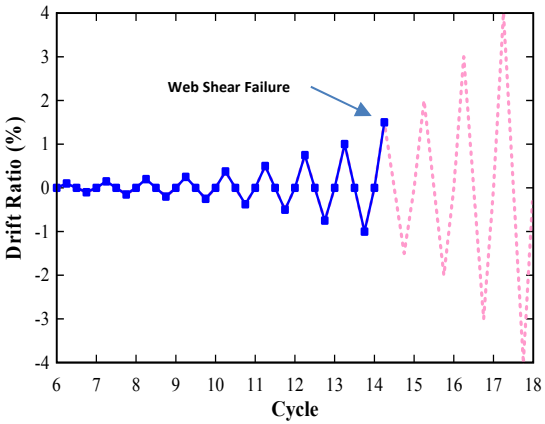

Loading history

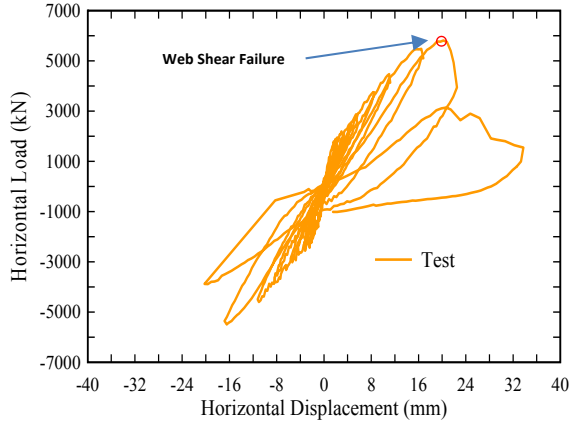

Horizontal load vs. displacement curve

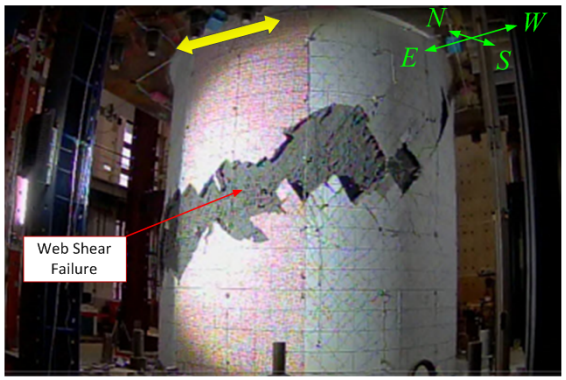

Web shear failure
(Cycle 14 – Drift 1.5%)

5. Nuclear Containment Vessels

Finite element models of RCCV specimens

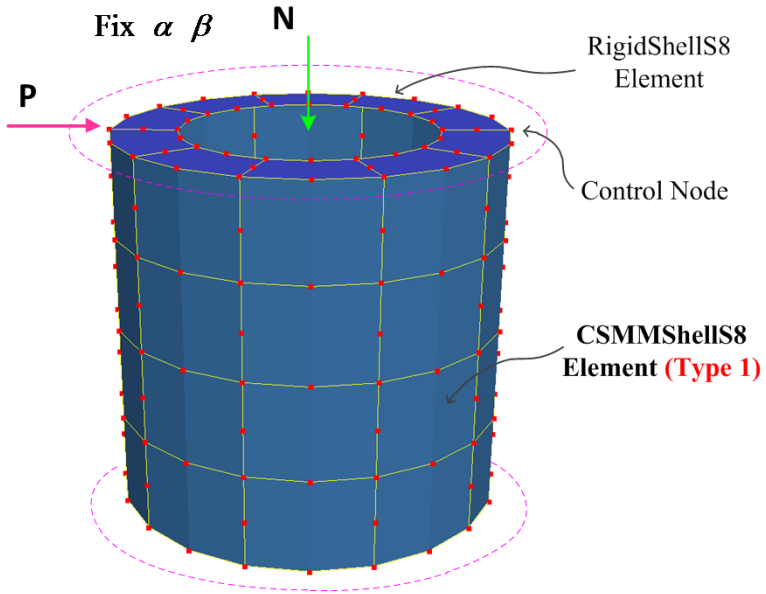

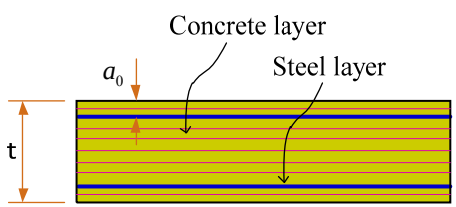

Specimen No. 1

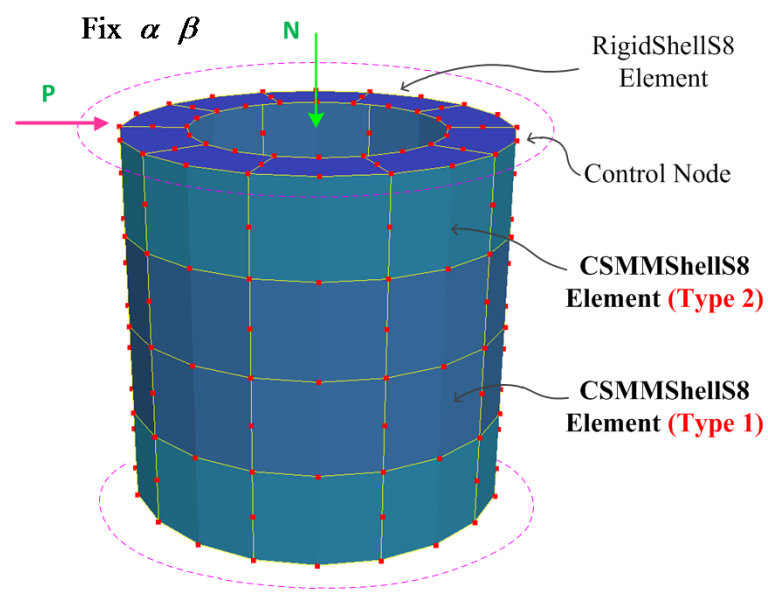

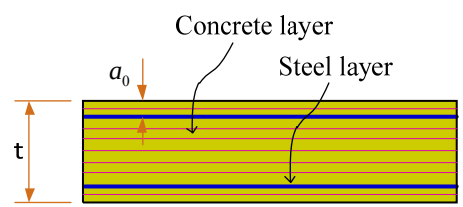

Specimen No. 2

Element Type	ρ_v	ρ_h
CSMMShellS8 Element (Type 1)	2 %	2 %
CSMMShellS8 Element (Type 2)	4 %	2 %

5. Nuclear Containment Vessels

Comparisons of analytical and experimental results

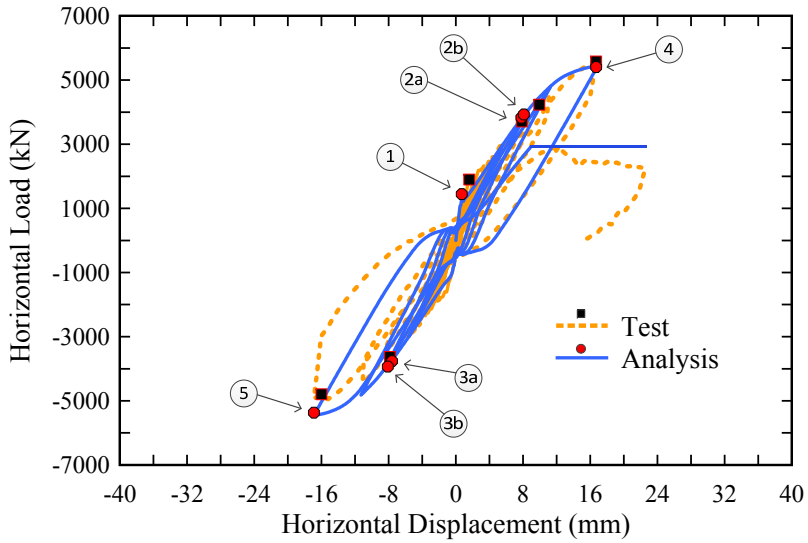

Horizontal load versus displacement curve of Specimen No. 1

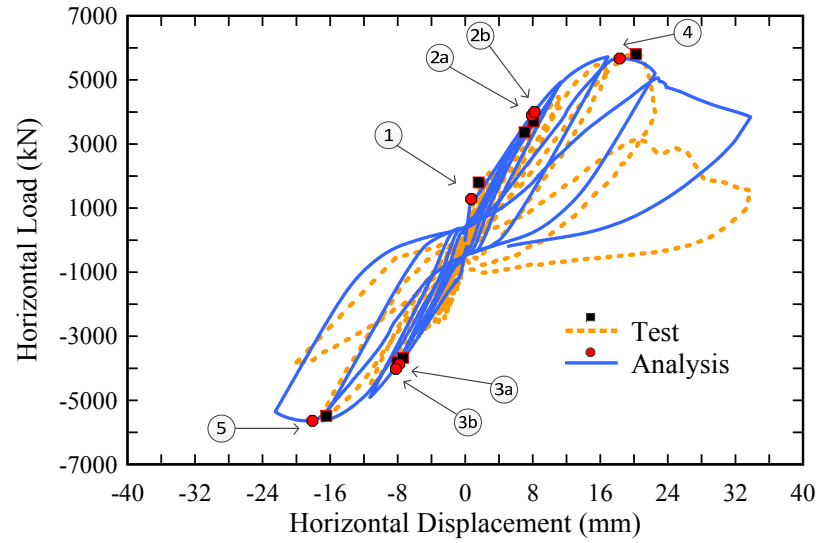

Horizontal load versus displacement curve of Specimen No. 2

Critical Points on the load vs. displacement curves

Points	Status
1	First cracking of concrete
2a	First yield of vertical steel bars in the positive direction
2b	First yield of horizontal steel bars in the positive direction
3a	First yield of vertical steel bars in the negative direction
3b	First yield of horizontal steel bars in the negative direction
4	Peak load in the positive direction
5	Peak load in the negative direction

Experimental Results

Specimen	Loading Direction	Δ_y (mm)	P_y (kN)	Δ_{max} (mm)	P_{max} (kN)	μ
1	(+)	7.84	3706	16.7	5580	2.13
	(-)	7.86	3634	16.0	4794	2.04
2	(+)	7.04	3363	20.2	5805	2.87
	(-)	7.38	3675	16.5	5487	2.23

Analytical Results

Specimen	Loading Direction	Δ_y (mm)	P_y (kN)	Δ_{max} (mm)	P_{max} (kN)	μ
1	(+)	7.8	3829	16.7	5400	2.14
	(-)	7.6	3764	16.9	5367	2.22
2	(+)	7.9	3897	18.3	5669	2.31
	(-)	7.8	3873	18.1	5640	2.32

5. Nuclear Containment Vessels

Specimen No. 1

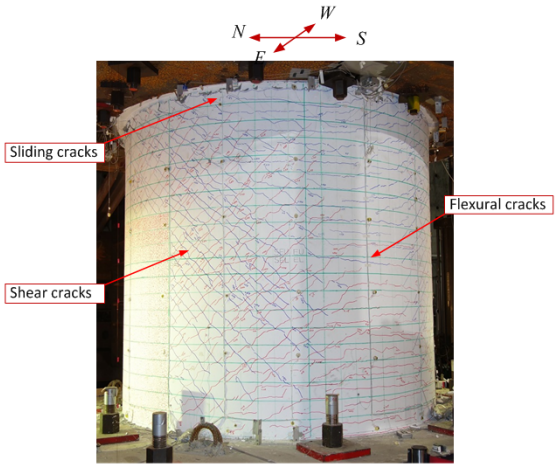

Experimental crack pattern of Specimen No. 1 (Drift 0.5%)

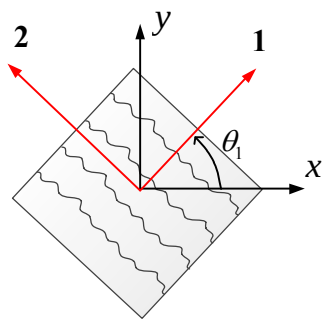

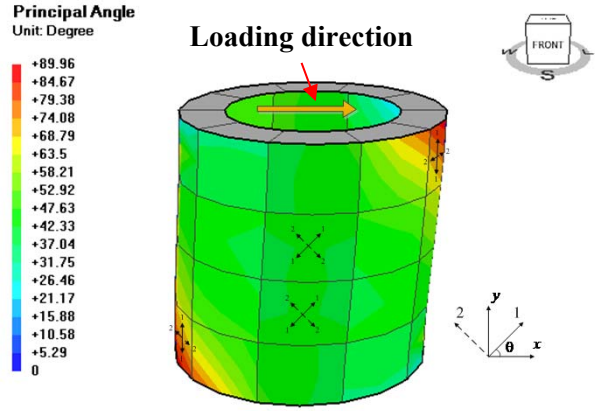

Contour of the angles between principal stress direction and local coordinate of Specimen No. 1 (Drift 0.5%)

Specimen No. 2

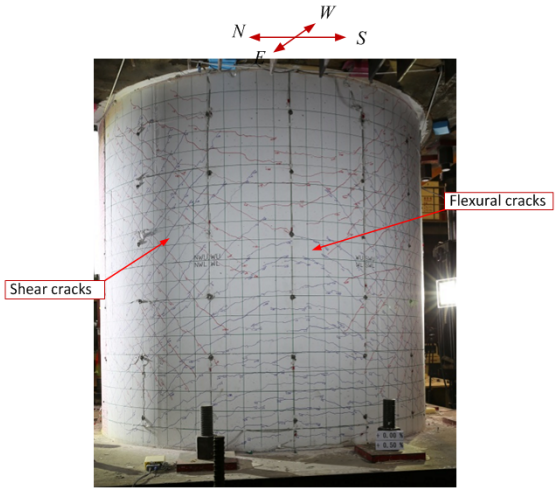

Experimental crack pattern of Specimen No. 2 (Drift 0.5%)

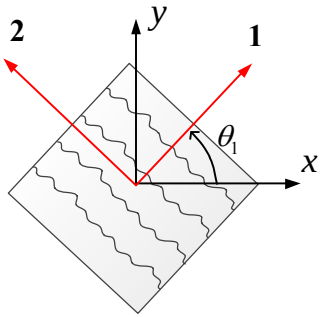

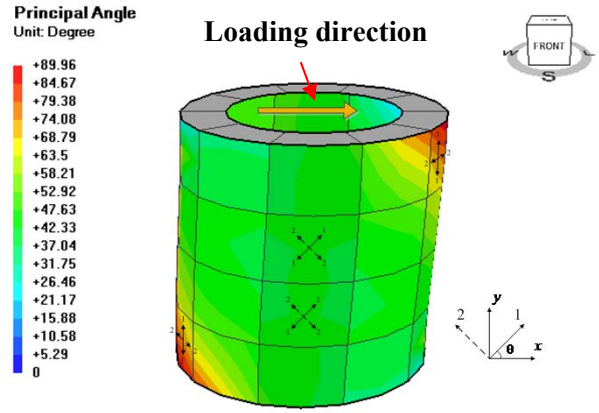

Contour of the angles between principal stress direction and local coordinate of Specimen No. 2 (Drift 0.5%)

5. Nuclear Containment Vessels

Contour of strains of the vertical steel bars in Specimen No. 1 at (First yield state)

Loading direction

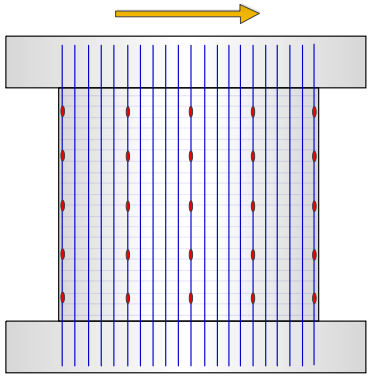

Strain gauge distribution on vertical steel bars

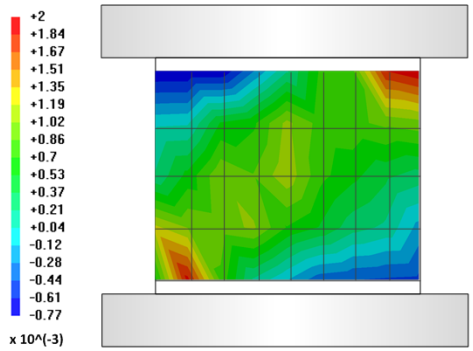

Experimental results

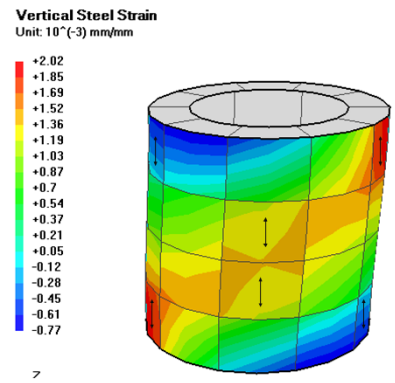

Analytical results

Contour of strains of the horizontal steel bars in Specimen No. 1 at (First yield state)

Loading direction

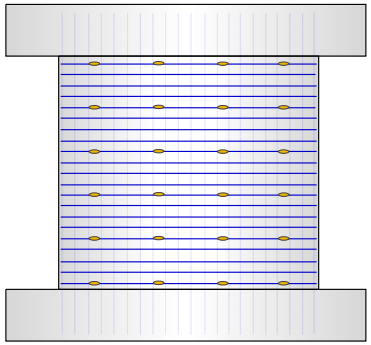

Strain gauge distribution on horizontal steel bars

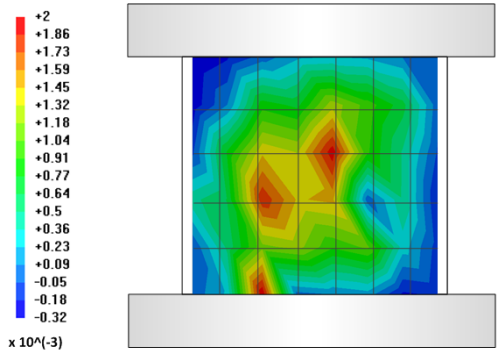

Experimental results

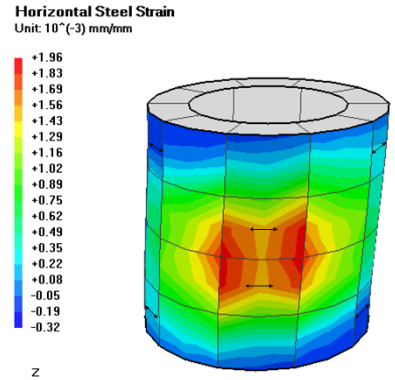

Analytical results

5. Nuclear Containment Vessels

Contour of strains of the vertical steel bars in Specimen No. 2 at (First yield state)

Loading direction

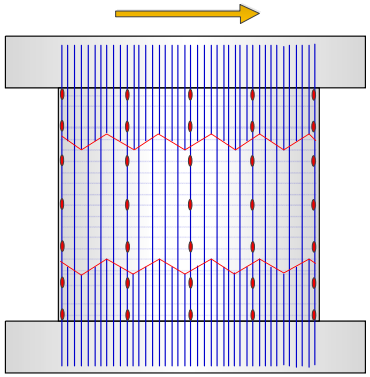

Strain gauge distribution on vertical steel bars

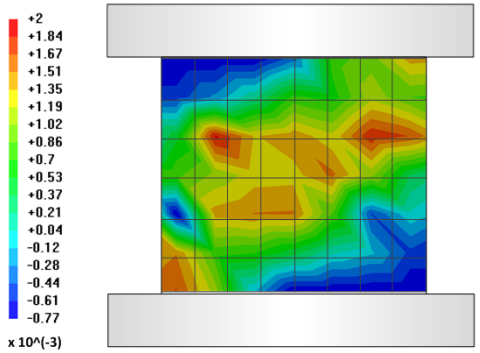

Experimental results

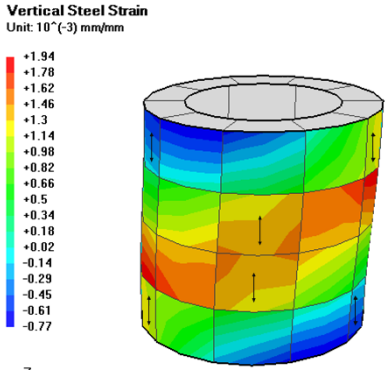

Analytical results

Contour of strains of the horizontal steel bars in Specimen No. 2 at (First yield state

Loading direction

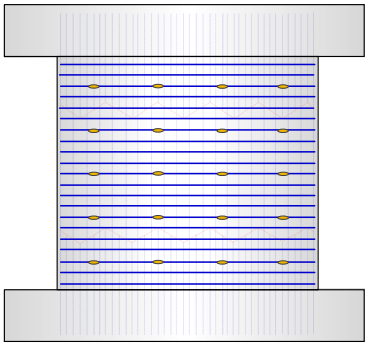

Strain gauge distribution on horizontal steel bars

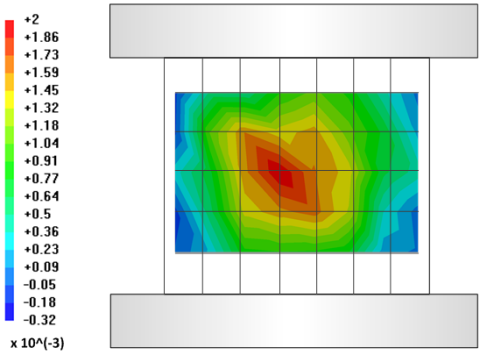

Experimental results

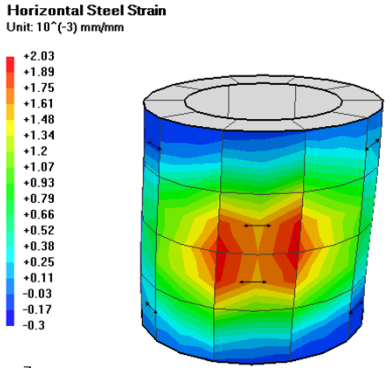

Analytical results

5. Nuclear Containment Vessels

Contour of strains of the vertical steel bars in Specimen No. 1 at (Peak load state)

Loading direction

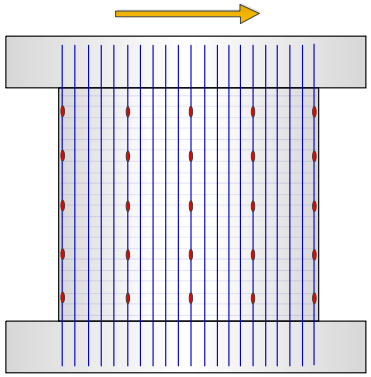

Strain gauge distribution on vertical steel bars

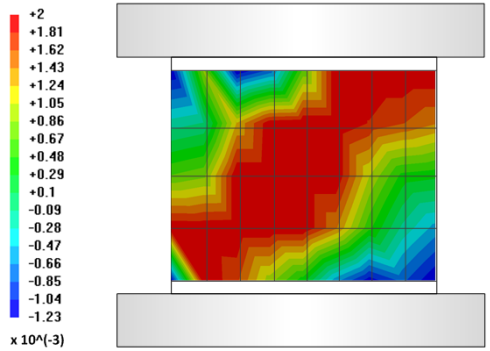

Experimental results

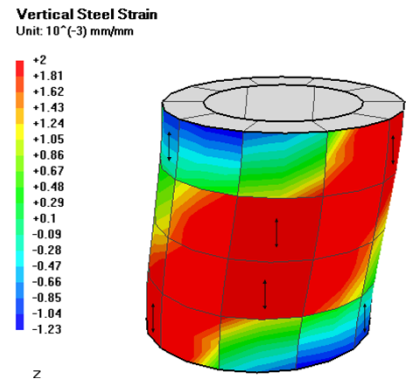

Analytical results

Contour of strains of the horizontal steel bars in Specimen No. 1 at (Peak load state)

Loading direction

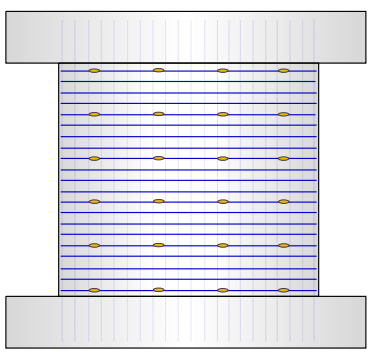

Strain gauge distribution on horizontal steel bars

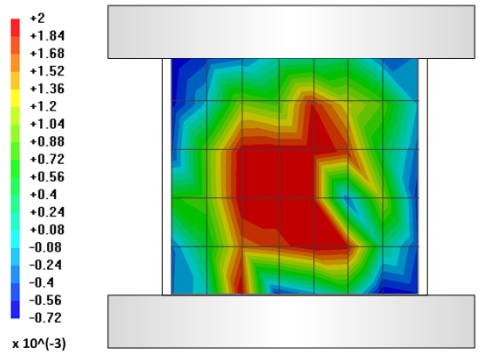

Experimental results

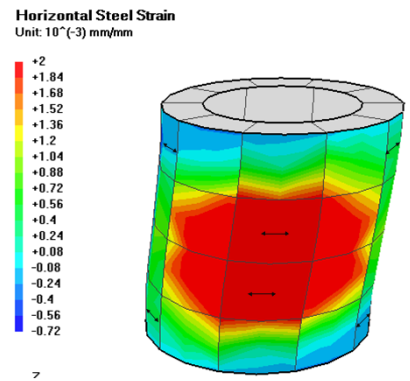

Analytical results

5. Nuclear Containment Vessels

Contour of strains of the vertical steel bars in Specimen No. 2 at (Peak load state)

Loading direction

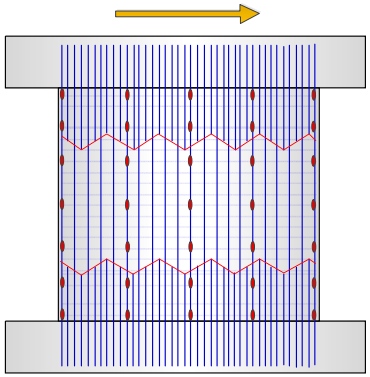

Strain gauge distribution on vertical steel bars

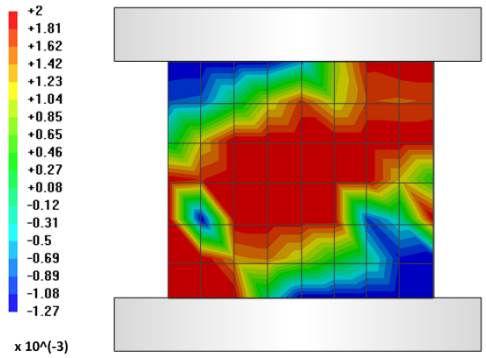

Experimental results

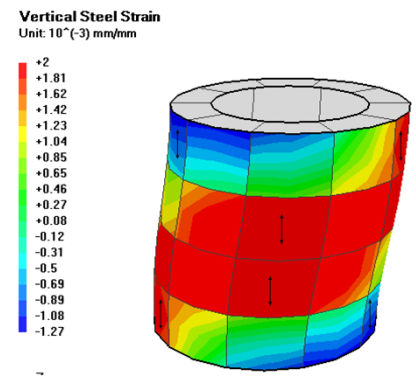

Analytical results

Contour of strains of the horizontal steel bars in Specimen No. 2 at (Peak load state)

Loading direction

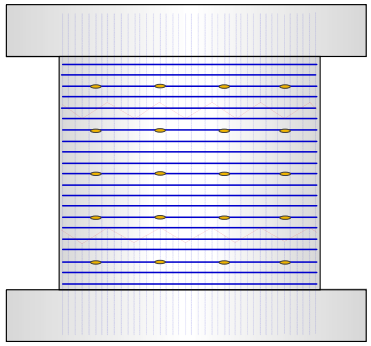

Strain gauge distribution on horizontal steel bars

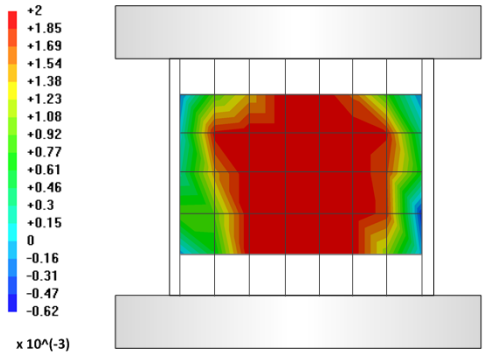

Experimental results

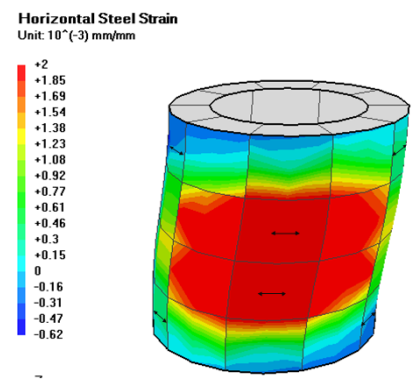

Analytical results

5. Nuclear Containment Vessels

Study of Sliding Shear Failure Mechanism in Specimen No. 1

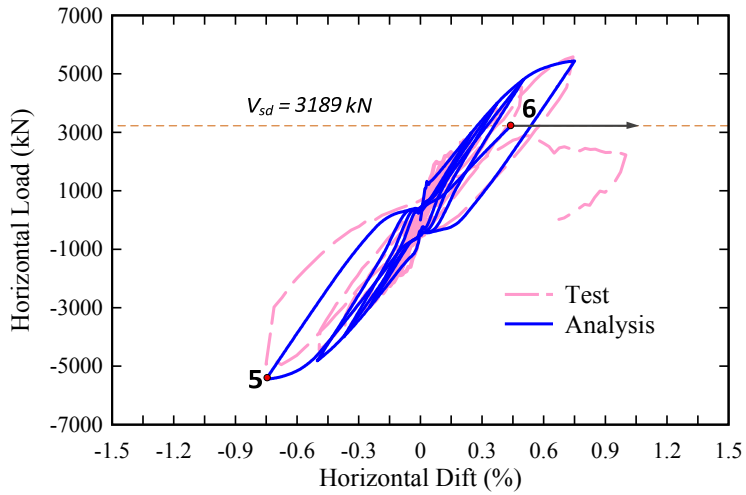

Horizontal load vs. displacement curve

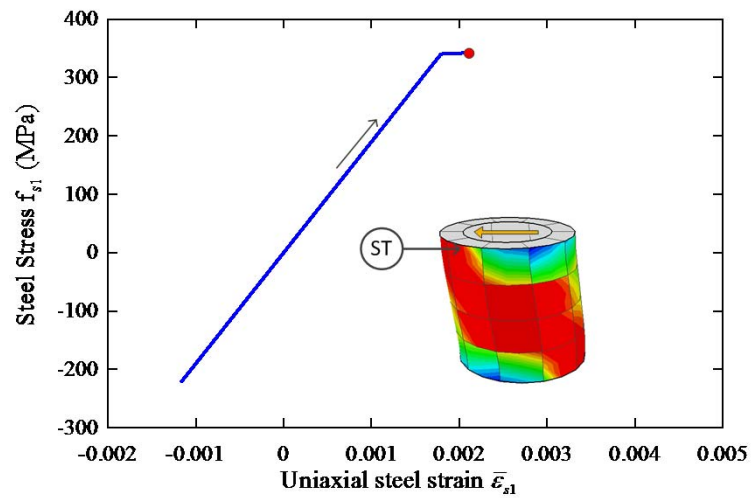

Stress-strain curve of vertical steel bar at point ST (Stage: Point 5 on the load vs. displacement curve)

$$A_{sw} = \rho A_c = \rho \frac{\pi}{4}\left(D^2 - d^2\right)$$

$$A_{sw} = 0.02\ \frac{\pi}{4}\left(2500^2 - 2200^2\right)$$

$$A_{sw} = 22150\ (mm^2)$$

$$V_{sd} \ \square\ 0.4 \times 22150 \times 360 = 3189\ \ kN$$

Calculation of sliding shear capacity

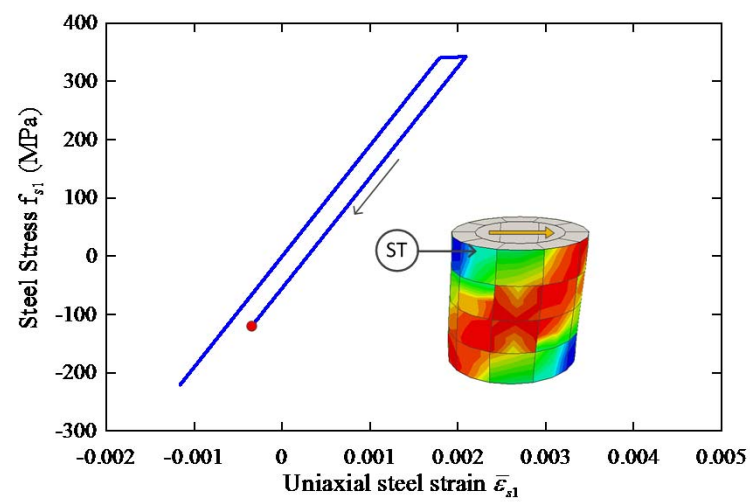

Stress-strain curve of vertical steel bar at point ST (Stage: Point 6 on the load vs. displacement curve)

5. Nuclear Containment Vessels

Study of Web Shear Failure Mechanism in Specimen No. 2

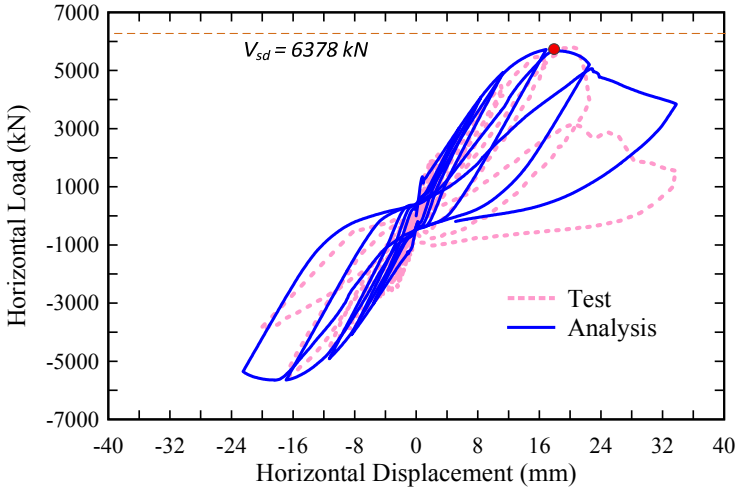

Horizontal load vs. displacement curve

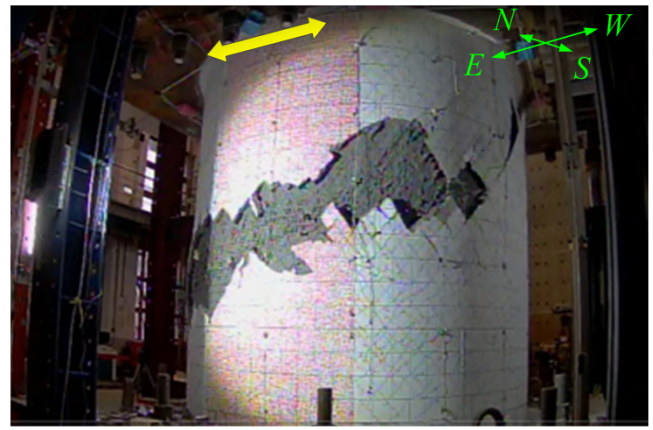

Web shear failure
(Cycle 14 – Drift 1.5%)

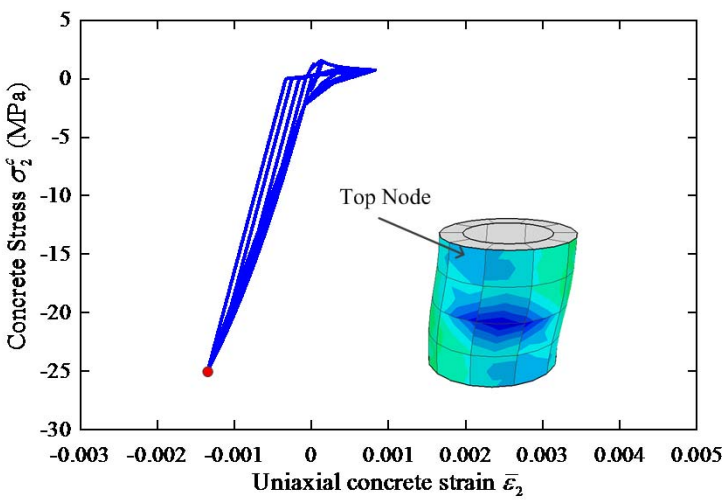

Stress-strain curve of concrete in principal direction at the top of the specimen (Peak load stage)

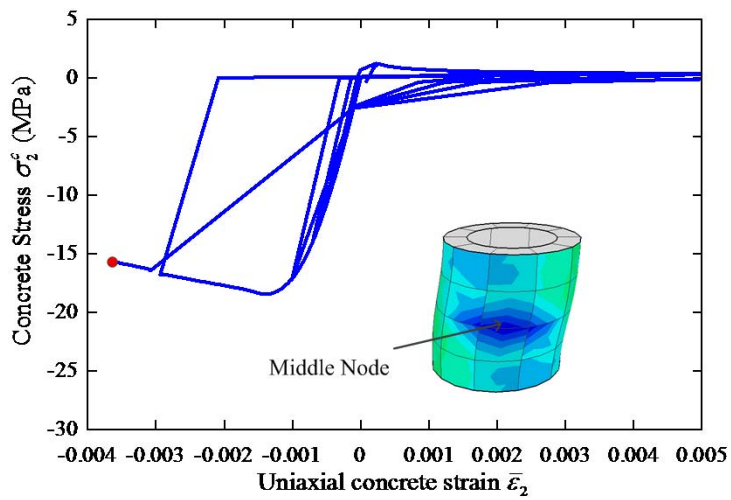

Stress-strain curve of concrete in principal direction at the middle of the specimen (Peak load stage)

7. Conclusions

- Using CSMM, a degenerated shell element with layered approach was developed. The developed shell element and the proposed analysis procedure were implemented into OpenSees to create a finite element analysis program SCS-3D, which can be used to predict the inelastic behavior of three-dimensional RC structures.

- Two 1/13-scale nuclear containment vessel specimens were designed and tested under revered cyclic loading. The first specimen failed by the sliding shear mode, and the second specimen failed by the web shear mode.

- The finite element program SCS-3D can predict the inelastic behavior of the RCCV specimens with good accuracy, including the cracking patterns, the first yielding points, the yielding distributions of the steel bars, the hysteretic loops of the load and displacement curve and failure modes.

Thanks for Your Attention.

UNIVESITY of
HOUSTON

Dept. of Civil and Environmental Engineering